Biogeosciences Discuss., https://doi.org/10.5194/bg-2017-570
Manuscript under review for journal Biogeosciences
Discussion started: 15 January 2018
© Author(s) 2018. CC BY 4.0 License.

Diazotrophic *Trichodesmium* influence on ocean color and pigment composition in the South West tropical Pacific

Cécile Dupouy[1*], Robert Frouin[2], Marc Tedetti[1], Morgane Maillard[1], Martine Rodier[3], Fabien Lombard[4], Lionel Guidi[4], Marc Picheral[4], Solange Duhamel[5], Bruno Charrière[6], Richard Sempéré[1]

[1] Aix Marseille Univ, Université de Toulon, CNRS, IRD, MIO UM 110, 13288, Marseille, France
[2] Scripps Institution of Oceanography, University of California San Diego, La Jolla, California, USA
[3] Environnement Insulaire Océanien (EIO), UMR 241 (Université de Polynésie Française, Institut de Recherche pour le Développement, Institut Louis Malardé, IFREMER), Centre IRD de Tahiti, BP 529, 98713 Papeete, French Polynesia
[4] Sorbonne Universités, UPMC Université Paris 06, CNRS, Laboratoire d'Océanographie de Villefranche (LOV), Observatoire Océanologique, 06230 Villefranche-sur-Mer, France
[5] Lamont Doherty Earth Observatory, Columbia University, Palisades, New York, USA
[6] CNRS, Cefrem, Université de Perpignan. 52, av. Paul Alduy 66860, Perpignan Cedex, France
* Aix Marseille Université, CNRS/INSU, Université de Toulon, IRD, Mediterranean Institute of Oceanography (MIO) UM 110, 98848, Nouméa, New Caledonia

[*] Corresponding author: Aix Marseille Univ, Université de Toulon, CNRS, IRD, MIO UM 110, 13288, Marseille, France : cecile.dupouy@ird.fr

- **Keywords:** *Trichodesmium*, chlorophyll, pigments, normalized water leaving radiances, inherent optical properties, South West tropical Pacific

Abstract

We assessed the influence of the marine diazotrophic cyanobacterium *Trichodesmium* on the bio-optical properties of South West tropical Pacific waters (18-22 °S, 160 °E-160 °W) during the February-March 2015 OUTPACE cruise. We performed measurements of backscattering and absorption coefficients, irradiance, and radiance, in the euphotic zone, and took Underwater Vision Profiler 5 (UPV5) pictures for counting the largest *Trichodesmium*

Biogeosciences Discuss., https://doi.org/10.5194/bg-2017-570
Manuscript under review for journal Biogeosciences
Discussion started: 15 January 2018
© Author(s) 2018. CC BY 4.0 License.

spp colonies. Pigment concentrations were determined by fluorimetry and by high performance liquid chromatography and picoplankton abundance by flow cytometry. Trichome concentration was estimated from pigment algorithms and validated by surface visual counts. In result, the large colonies were well correlated to the trichome concentration estimates (though with a large factor of 600 to 900, due to aggregation processes). Large *Trichodesmium* abundance was always associated with particulate absorption at a peak of mycosporine-like amino acid absorption, and high particulate backscattering, but not with high fluorescence, high chlorophyll-a concentration, or blue particulate absorption in the water column. Along the West to East transect, *Trichodesmium* together with *Prochlorococcus* represented the major part of total chlorophyll and the other groups were negligible. *Trichodesmium* contribution to chlorophyll was the highest in the Melanesian Archipelago around New Caledonia and Vanuatu, progressively decreased to the vicinity of the Fiji Islands, and reached a minimum in the South Pacific gyre where the contribution of *Prochlorococcus* was maximum. At the frontal LDB, *Trichodesmium* and *Prochlorococcus* has almost same contributions. The relationship between normalized water-leaving radiance, in the ultraviolet and visible domains, nL_w, and chlorophyll was generally similar to that found in the Eastern tropical at BIOSOPE. Principal component analysis (PCA) of OUTPACE data showed that nL_w were strongly correlated to chlorophyll except in the green and yellow domains. These results, as well as differences in the PCA of BIOSOPE data, suggested that nL_w variability in the green and yellow during OUTPACE was influenced by other variables, associated with *Trichodesmium* presence as the backscattering coefficient, phycoerythrin fluorescence, and/or zeaxanthin absorption. *Trichodesmium* detection should then involve examination of nL_w at the green and yellow wavelengths.

1 Introduction

The ecological importance of filamentous diazotrophs (*Trichodesmium* spp. in particular) in the archipelago region of the South West tropical Pacific (SWTP) has long been pointed out (Dandonneau and Nyang, 2007). *Trichodesmium* spp. have to be taken into account for the estimation of the global oceanic nitrogen and carbon cycles (Capone and Carpenter, 1997; Bonnet et al., 2017; Dutheil et al., this issue). In the past decade, efforts have been made to extract abundances of different phytoplanktonic taxonomic groups from ocean color data (Blondeau-Patissier et al., 2014; Bracher et al., 2017). Other attempts have been made to get remote sensing estimates of the abundance and diazotroph activity of *Trichodesmium* at a global scale (Westberry and Siegel, 2005; McKinna et al., 2011; Dupouy et al., 2011; McKinna, 2015). Satellite detection of *Trichodesmium* is facilitated when concentration at the sea surface is high, leading to a building of mat larger than a satellite pixel. These mats induce a high reflectance in the near infrared, a “red edge”, which can easily be observed (Hu et al.,

© Author(s) 2018. CC BY 4.0 License.

2010; Dupouy et al., 2011; McKinna et al., 2011; Gower et al., 2014; McKinna, 2015; Rousset et al., this issue). Detection becomes more difficult when *Trichodesmium* concentrations are at non-bloom or sub-bloom abundance, i.e. when colonies are distributed throughout the water column and mixed with other species. Using empirical statistical approach, De Boissieu et al. (2014) determined that at sufficient concentration level, these filamentous diazotrophs can be distinguished from other groups. This complements empirical parameterizations that were used to derive the vertical distribution of different phytoplankton groups (microplankton, nanoplankton, and picoplankton) using High Performance Liquid Chromatography (HPLC) diagnostic pigments and surface chlorophyll a (Chla) determination from space (Uitz et al., 2006; Ras et al., 2008; Brewin et al., 2011).

In order to validate *Trichodesmium* discrimination algorithms, and to improve the knowledge of the influence of *Trichodesmium* spp. on apparent (AOPs) and inherent (IOPs) optical properties of seawater, accurate field determinations are required. E.g., it is necessary to measure the normalized water-leaving radiance [$nL_w(\lambda)$ in W m^{-2} sr^{-1}], i.e., the radiance that emerge from the ocean in the absence of atmosphere, with the Sun at zenith, at the mean Earth-Sun distance (Gordon, 2005). $nL_w(\lambda)$ is governed by two main IOPs (Mobley 1994; Kirk, 1994): volume absorption [$a(\lambda)$ in m^{-1}] and volume backscattering [$b_b(\lambda)$ in m^{-1}] coefficients. IOPs are controlled by the concentrations of optically active components in a volume of water, which include phytoplankton and colored detrital matter (CDM), the latter being composed by non algal particulate matter (NAP) and chromophoric dissolved organic matter (CDOM). If AOPs are well related to phytoplankton pigments in Case I oceanic waters (Morel and Maritorena, 2001, Morel et al., 2007), this relationship might be modified by the presence of *Trichodesmium* (with moderate Chla concentrations < 1 mg m^{-3}). As summarized in Westberry and Siegel (2005), *Trichodesmium* displays unique optical properties that may allow their detection: (1) a strong absorption in the ultraviolet (UV) domain related to the presence of mycosporin like amino-acids (Subramaniam et al., 1999a; Dupouy et al, 2008), (2) a higher relative reflectance near 570 nm due to phycoerythrin fluorescence (Borstad et al., 1992; Subramaniam et al., 1999b), and (3) an increased backscattering across all wavelengths caused by the index of refraction change within intracellular gas vacuoles (Borstad et al., 1992; Subramaniam et al., 1999b; Dupouy et al., 2008).

The SWTP between New Caledonia and the Tonga trench is particularly rich in *Trichodesmium* colonies during summer (Dupouy et al., 1988; 2000; 2011; Biegala et al., 2014) and this richness further enhanced during the positive phase of the ENSO in 2003

Biogeosciences Discuss., https://doi.org/10.5194/bg-2017-570
Manuscript under review for journal Biogeosciences
Discussion started: 15 January 2018
© Author(s) 2018. CC BY 4.0 License.

(Tenorio et al., in press). Using bio-optical measurements, this study aims (1) to describe several AOPs and IOPs of interest in the UV and visible domains of SWTP waters, as well as pigments, and abundance of all phytoplanktonic cells including large and smaller *Trichodesmium* colonies and picoplankton, (2) to determine the influence of *Trichodesmium* spp. on *in situ* measurements of ocean color, and absorption and backscattering coefficients. For this purpose, we used identical measurements than those implemented in the tropical oligotrophic ocean during the BIOSOPE cruise (Tedetti et al., 2007; 2010).

2 Material and methods

2.1 Study area

The "Oligotrophy from Ultra-oligoTrophy PACific Experiment (OUTPACE)" cruise was conducted on board the RV L'Atalante from 21 February to 31 March 2015 in the South West tropical Pacific Ocean (Table 1; Fig. 1). *In situ* measurements and water sampling were performed at fifteen stations along a 4000-km transect extending from the mesotrophic waters of the Melanesian Archipelago (MA, SD1 to SD6), near New Caledonia and Vanuatu to the Fijian archipelago (FI, SD7 to SD12), between Fiji and Tonga, and to the extreme eastern end in the hyper-oligotrophic waters of the South Pacific East of Tonga Trench in the Gyre (SPG, SD12 to SD15). General biogeochemical and hydrographic characteristics of the waters along this transect are described in Moutin et al. (this issue).

2.2. Radiometric measurements and determination of $nL_w(\lambda)$, $K_d(\lambda)$ and $Z_{10\%}(\lambda)$ values

At each station, two or more profiles of downward irradiance [$E_d(Z, \lambda)$ in $\mu W\ cm^{-2}\ nm^{-1}$] and upward radiance [$L_u(Z, \lambda)$ in $\mu W\ cm^{-2}\ nm^{-1}\ sr^{-1}$] were made at each station around solar noon using a Satlantic MicroPro free-falling profiler equipped with OCR-504 downward irradiance and upward radiance sensors with UV-B (305 nm), UV-A (325, 340 and 380 nm) and visible (412, 443, 490 and 565 nm) spectral channel, as further described in Tedetti et al. (2010). The MicroPro free-fall profiler was operated from the rear of the ship and deployed 30 m away to minimize the disturbances of the ship. Surface irradiance [$E_s(\lambda)$ in $\mu W\ cm^{-2}\ nm^{-1}$] was concomitantly measured at the same wavelengths on the ship deck using other OCR-504 sensors to account for the variations of cloud conditions during the cast. Satlantic, Inc. surface and in-water radiometers were calibrated before the cruise. Mostly cloudy sky conditions existed during the profiles (only a few acquisitions were made under clear skies),

© Author(s) 2018. CC BY 4.0 License.

and at SD5 at 17:30-19:00 they were made under a heavy shower. SD3, SD4, and SD13 profiles were not available (night stations). Details of the casts can be found in Appendix A. Determination of $nL_w(\lambda)$ was conducted from values of $L_u(Z, \lambda)$, diffuse attenuation coefficient for upward radiance ($K_L(\lambda)$ in m^{-1}), water-leaving radiance [$L_w(Z, \lambda)$] and $E_s(\lambda)$ (see calculations in Appendix A). The $nL_w(\lambda)$ data presented in this study are average values of two to three upward radiance casts (coefficient of variation < 8% for all the stations concerned). Diffuse attenuation coefficient for downward irradiance ($K_d(\lambda)$ in m^{-1}) was determined using $E_d(Z, \lambda)$ and $E_s(\lambda)$ values (Appendix A).

The first optical depth corresponding to the surface layer observed by the satellite ocean color instruments (Kirk, 1994) [$Z_{10\%}(\lambda)$ in m] was extrapolated from $K_d(\lambda)$ and calculated as $\ln(10)/K_d(\lambda)$. In this study, the integrated concentrations of the different microorganisms between the surface and the first optical depth were used to determine the relationship between these concentrations and $nL_w(\lambda)$ values.

2.3 Water sampling

Seawater samples were collected during the noon cast of each station at different depths using 12-L Niskin bottles for the determination of various parameters. For the determination of Chla concentration and particulate (phytoplankton + NAP) absorption coefficient [$a_P(\lambda)$], samples were collected at depths corresponding to different % of PAR (i.e., 75, 54, 36, 10, 1, 0.1%) and filtered [288 mL for Chla and 2.25 L for $a_P(\lambda)$] through 25-mm Whatman GF/F filters. After filtration, the latter were immediately stored at -80 °C (liquid N_2) in Nunc® cryogenic vials until analysis. Liposoluble pigments were sampled at all depths (LOV laboratory data, OUTPACE data basis, J. Ras). In addition, samples were taken in duplicate at surface and Deep Chlorophyll Maximum (DCM) as part of a NASA satellite validation program. For this, 3 to 4.5 L of seawater was filtered onto 25-mm Whatman GF/F filters, which were further stored in liquid N_2 until analyses at NASA. Watersoluble pigments (phycoerythrin, PE) concentration were determined for the >10 µm size fractions, therefore 4.5 L of seawater were filtered onto 47-mm Nuclepore filters with pore sizes 10-µm and stored in Nunc® cryogenic vials. Filters were preserved at -80 °C until analysis at the laboratory (IRD French Polynesia). For the determination of surface picoplanktonic population abundances (Bock et al., this issue), water samples were fixed with paraformaldehyde (final concentration of 0.2%) immediately after sampling, flash frozen in liquid nitrogen, and stored at -80°C in Nunc® cryogenic vials until analysis. For the

© Author(s) 2018. CC BY 4.0 License.

determination of CDOM absorption, 200 mL of seawater were stored in SCHOTT® glass bottles precombusted (450°C, 6 hours) and rinsed twice with HCL before use, and immediately filtered on 0.2-µm Micropore filters on Nalgene filtration units rinsed twice with HCL before each station.

Pump samples were also taken all along three transects in order to increase the frequency of both pigments and IOPs' surface measurements (Chla, HPLC-NASA) in areas characterized by important *Trichodesmium* spp. surface slicks : the "Simbada" transect, with 7 pump samples between SD3 and SD4 in the Melanesian archipelago (MA) (Appendix B), and the High Frequency HF1 transect (31samples), around LDA, and the HF2 transect in the Fijian archipelago (FI) near LDB (42 samples) (Dupouy, OUTPACE data basis). Besides radiometric measurements and water sampling, *in situ* measurements were also conducted for the determination of *Trichodesmium* spp. colonies and backscattering coefficients (see below).

2.4 Phytoplankton abundance

2.4.1 FTL$_{Trichodesmium}$ abundance: large *Trichodesmium* spp. colonies

An Underwater Vision Profiler 5 (UVP5), serial number Sn003, pixel size ca. 0.147 mm; (Picheral et al., 2010) was deployed fixed to the CTD. The device emitted flashes of red LED light that illuminates 0.95 L of water. Images of all particles within the illuminated area were recorded and analyzed for abundances in defined size ranges. Objects larger than 30 pixels were saved and uploaded on ecotaxa (http://ecotaxa.obs-vlfr.fr/prj/37) and further analyzed by a taxonomist. From 190074 objects recovered, 100342 were identified as "fiber tricho like *Trichodesmium*" (FTL$_{Trichodesmium}$)", i.e. all particles of *Trichodesmium* with fusiform-shape (tuff form) and round-shape (puff form) colonies from < 200 µm to 2-5 mm in size. FTL$_{Trichodesmium}$ is assumed to be mostly *Trichodesmium* colonies with the risk that a small quantity of fibers is interpreted as diatoms chains. Contrary to a classical counting at the microscope, no abundance of free filaments is available, although these filaments represent often a significant part of the *Trichodesmium* assemblage (Carpenter et al., 2004). The FTL$_{Trichodesmium}$ abundance is calculated in N m^{-3} at 5-m depth intervals (Picheral et al., 2010) providing FTL$_{Trichodesmium}$ "vertical concentrations" at each cast. Surface FTL$_{Trichodesmium}$ abundance was selected for the surface at each station of the transect. The FTL$_{Trichodesmium}$ abundance at 5m water depth was generally underestimated compared to that at 10-m and 15-m depths (possibly due to smaller size of colonies). Therefore, the value at 10 m was selected

© Author(s) 2018. CC BY 4.0 License.

as representative of the abundance of the surface layer. As different $FTL_{Trichodesmium}$ abundance profiles were done during the day (from 1 to 5 depending on the station), a daily average at 10 meters of the $FTL_{Trichodesmium}$ abundance was made. Daily average, maximum value of the day, and the $FTL_{Trichodesmium}$ abundance of the noon profile (i.e. the nearest from the time of the optical profile) showed no statistical difference. For the long duration stations, an average on 7 days of the 10m-$FTL_{Trichodesmium}$ abundance was calculated as representative of the station.

As an attempt to estimate a trichome concentration, photographies with a Dino-Lite hand-held Digital Microscope covering the totality of the filtered surface on the GF/F filters used for absorption measurements were used. Colonies were first visually enumerated. The uncertainty on this colony visual enumeration was estimated at 20%. For estimating trichome concentration (L^{-1}), a number of 10 trichomes per colony was arbitrarily chosen (representing an average of each size class and shapes; Dupouy et al., in prep.)

2.4.2 Picoplankton

Surface picoplankton population abundances were estimated by flow cytometry using a BD Influx flow cytometer (BD Biosciences, San Jose, CA, USA). *Prochlorococcus* (Proc), *Synechochoccus* (Syn) and picoeucaryotes (peuk) were enumerated using the red and orange fluorescence, while non-pigmented bacteria and protist groups were discriminated in a sample aliquot stained with SYBR Green I DNA dye, as described in Bock et al (this issue). Using a forward scatter detector with the "small particle option" and focusing at 488 and 457 nm (200 and 300 mW solid state, respectively) laser into the same pinhole greatly improved the discrimination between the dim signal from Pro at the surface and background noise in unstained samples. Nanoeucaryotes were not further differentiated from peuk. Cell abundances of Proc, Syn, peuk and bacteria showed a vertical and uniform abundance distribution due to their mixing in the 0-30m layer (Bock et al., this issue).

2.5 Chlorophyll a, phycoerythrin and pigment analyses

For Chla determination by the fluorimetric method, filters were extracted with 5 mL methanol in darkness over a 2 h period at 4 °C and quantified using a Trilogy Turner fluorometer according to Le Bouteiller et al. (1992) for samples collected over the entire 0-150 m water column. Surface HPLC pigments (surface, DCM) were measured according to the NASA protocol and provided monovivyl-Chla (MV-Chla), divinyl-Chla (DV-Chla), and all accessory pigments, photosynthetic and photoprotective carotenoids (Hooker et al., 2012).

© Author(s) 2018. CC BY 4.0 License.

PE was extracted in 50/50 glycerol/phosphate buffer. Quantification of this pigment were obtained from the area below the fluorescence excitation curve, using a calibrating procedure previously described (Wyman, 1992; Lantoine and Neveux 1997; Neveux et al., 2006). An estimate of the relative contribution of each phytoplankton group in terms of Chla was calculated in Excel from the pigment/Chla ratio found in CHEMTAX (Higgins et al. 2011). Furthermore, pigment ratios were also used to estimate the relative importance of different size categories in terms of Chla pico-, nano- and micro-plankton (Ras et al., 2008). The proportion of Proc to total Chla (TChla) biomass was estimated from the DV-Chla/TChla ratio. It usually represents a high proportion due of its high abundance despite of its small size (Grob et al., 2008).

2.6 *Trichodesmium* concentration algorithms from pigments

As true microscopic determination of *Trichodesmium* abundance was not realized at each station during the OUTPACE cruise, we used algorithms to derive trichome concentrations from pigment concentrations (chlorophylls, zeaxanthin, PE>10µm) and flow cytometric cell countings. Using a constant PE concentration per trichome (196 pg trichome^{-1}) and a constant Chla per trichome (100 pg cell^{-1}) as in Tenorio et al. (in press), calculations of trichome concentration (L^{-1}) could be done both from PE > 10 µm, or Chla > 10 µm, assuming that other autotrophic organisms have a negligible contribution in this large size fraction. As fractionated Chla (Chla > 10 µm), however, was not available for OUTPACE, Total MV-Chla was used, which corresponds to the sum of Chla from Syn and *Trichodesmium*, and all eukaryotic phytoplankton cells (pico-, nano-, and microphytoplankton), to estimate MV-Chla from other components of the autotrophic community and subtract them from the Total MV-Chla. MV-Chla associated with Syn and peuk was estimated using measured cell concentrations and the Chla per cell values obtained on cultures grown at high light intensity (Laviale and Neveux, 2011), i.e., 1.2 fg cell^{-1} for Syn and 10 fg cell^{-1} for peuk (assuming a concentration intermediate between the one of *Micromonas pusilla* and *Ostreococcus*). The zeaxanthin from *Trichodesmium* spp. was also estimated from total zeaxanthin using constant sizes for Syn and Peuk Laviale and Neveux (2011) and pigments/Chla ratios from Carpenter et al. (1993). We compared then estimations of *Trichodesmium* from these pigment algorithms to FTL$_{Trichodesmium}$ abundance and trichome concentration estimated from visual counts.

© Author(s) 2018. CC BY 4.0 License.

268 **2.7 Particulate and CDOM absorption and backscattering measurements**

269 Light absorption spectra were measured directly with filters soaked in filtered sea
270 water, by referencing them to an equally soaked empty filter. Measurements were done in
271 single-beam Beckman DU-600 spectrophotometer. Absorbance (optical density) spectra were
272 acquired between 300 and 800 nm in 2-nm steps. All spectra were shifted to zero in the
273 infrared by subtracting the average optical density between 750 and 800 nm. Finally, optical
274 densities were corrected for the pathlength amplification effect using and then converted into
275 the total particulate absorption coefficients [$a_P(\lambda)$ in m^{-1}] (Dupouy et al., 1997; 2003; 2008;
276 2010). The a_P(330 nm) to a_P(676 nm) ratio was calculated as an index of photoprotective
277 mycosporine-like amino acids (330 nm: absorption maximum of shinorine) from all
278 phytoplankton species (676 nm, absorption maximum of Chla), as in Ferreira et al. (2013).
279 CDOM absorption spectra were measured on board with a 200-cm pathlength liquid
280 waveguide capillary cell (LWCC, WPI) as described in Martias et al. (2018). Peaks at 350 nm
281 were visible in most of the CDOM spectra, except for LDB and SPG stations (not shown).

282 Backscattering coefficients were determined as described in Dupouy et al. (2010) from
283 a Hydroscat 6 (HOBILabs, Inc) at 6 wavelengths (412, 442, 510, 550, 620 and 676 nm). Only
284 stations SD1 to SD6 and LDA, days 1-5, were available, with the particulate backscattering
285 obtained by subtracting the backscattering coefficient of pure water (Morel, 1988).
286 Backscattering coefficients of surface oligotrophic waters (SD13, LDC, SD14, SD15) which
287 are supposed to depend deeply from TChla according to Huot et al. (2008) for the South East
288 Pacific, were deduced from Chla using a Look-Up Table of Diapalis data obtained in the
289 Loyalty Channel (Dupouy et al., 2010).

290

291 **2.8 Statistics**

292 Ocean Data View sections Schlitzer, R., Ocean Data View, http://odv.awi.de, 2016
293 was employed for the spatial representation of biogeochemical parameters over the vertical
294 (0-150m). The spatial interpolation/gridding of data was performed using Data-Interpolating
295 Variational Analysis (DIVA). Principal component analysis (PCA) was conducted on the
296 basis of Pearson's correlation matrices using XLSTAT 2011.2.05 for the surface stations, for
297 AOPs and TChla (HPLC).

Biogeosciences Discuss., https://doi.org/10.5194/bg-2017-570
Manuscript under review for journal Biogeosciences
Discussion started: 15 January 2018
© Author(s) 2018. CC BY 4.0 License.

298

3 Results

300

3.1 Distributions of $nL_w(\lambda)$, $K_d(\lambda)$ and $Z_{10\%}(\lambda)$

Along the OUTPACE transect, $nL_w(\lambda)$ showed a large range of values and spectral shape (Fig. 2a). In the UV (305–380 nm), violet (412 nm), and blue (443 and 490 nm) ranges, $nL_w(\lambda)$ were the lowest in the Melanesian archipelago's (MA), increasing towards the South Pacific Gyre (SPG) (SD14-SD15, LDC), which exhibited the highest $nL_w(\lambda)$. For all the wavebands, with the exception of the green one (565 nm), $nL_w(\lambda)$ at SD14 and LDC was higher than the 90th percentile, and $nL_w(\lambda)$ at SD9 and LDB were lower than the 10th percentile (Fig. 2b). Values of $nL_w(\lambda)$ in this violet-blue domain were similar than those measured in the most oligotrophic oceanic areas at the Eastern part of the OUTPACE transect (Tedetti et al., 2010). For example, in the center of the SPG (15°S-30°S, 126°W-86°W 160°W), $nL_w(412)$, $nL_w(443)$, and $nL_w(490)$ reached up to 4.5, 4, and 2 µW cm^{-2} sr^{-1} nm^{-1}, respectively for TChla concentrations < 0.022 mg m^{-3} and a DCM at 180 m. LDB had a characteristic spectrum with waters greener than all other stations (Fig. 2a). The low nL_w at LDB corresponds to a surface TChla accumulation of 1 mg m^{-3} on a surface physical front (Rousselet et al., this issue). This dark green color was astonishing from the ship deck while profiling of the Satlantic instrument. Moreover, the GF/F filters used for absorption showed an orange-yellow color when observed under the Dino-Lite microscope. Such color was not observed in the MA, and is typical of small picoplanktonic cells as Pro and Syn.

Table 1 displays $K_d(\lambda)$ values at the four UV wavelengths and for the whole PAR domain. For all stations, $K_d(\lambda)$ decreased from the UV-B to UV-A spectral domain (Table 1). From the MA to the FI, $K_d(325)$ was high from SD1 to SD6, then decreased from SD7 to SD12, and showed a peak at LDB, and minimum at the SPG stations. During the long duration stations, $K_d(325)$ variations (not shown) reflected those of TChla with values decreasing from day 1 to 5 at LDA (0.18 to 0.15 m^{-1}), at LDB (0.22 to 0.17 m^{-1}). They stayed stable at LDC. $K_d(PAR)$ (Table 1) showed the same distribution within the range 0.016 m^{-1} (LDC and SD14) to 0.028 m^{-1} (LDB). Typical values of $K_d(PAR)$ in oligotrophic waters associated to a deep DCM of 165 m and a TChla of 0.037 mg m^{-3} were measured at SD13-SD14-SD15-LDC. For comparison, such values are close to that found in South East Pacific during BIOSOPE cruise (08–35°S, 142–73°W) (Tedetti et al., 2007) and much lower than that reported for the oligotrophic water of NW Mediterranean Sea (Sempéré et al., 2015).

© Author(s) 2018. CC BY 4.0 License.

Maxima of $Z_{10\%}$(380) (Table 1, Fig. 3) were found in the FI at LDC and SD15 (100-120 m, for a TChla of 0.02 mg m^{-3}) and was comparable to those reported for the clearest natural waters in SPG (Tedetti et al., 2007). Conversely, stations exhibiting the lowest $Z_{10\%}$ (SD1, 40 m) were found in the MA and at the LDB frontal station in the FI (DCM of 41 m, TChla = 0.433 mg m^{-3}). The 1st optical depth determined in the UV-visible varied from 13 (LDB-Day3) to 28 m (SD14).

3.2 Pigment composition and abundance of phytoplanktonic groups

3.2.1 FTL*Trichodesmium* abundance derived from Underwater Vision Profiler

The UVP5 $FTL_{Trichodesmium}$ abundance showed a wide range of values along the transect SD1-SD15 (Fig. 4a, Table 1) in the SWTP. It was essentially concentrated in the upper 30 m although some were still visible below 30 m. The maximum was obtained at SD1 (4000 N m^{-3}) and rapidly dropped to 2000 N m^{-3} at SD2 to stabilize between 200 and 500 N m^{-3} at the east of SD4. It progressively decreased from West to East. Still visible at SD5 (170°E), it vanished at SD7, where the maximum of $FTL_{Trichodesmium}$ abundance was located deeper and finally disappeared between SD8 and SD11. A second maximum of $FTL_{Trichodesmium}$ abundance was found at LDB at 50 m with an exceptional value of 3500 N m^{-3} at Day1. The continuity of $FTL_{Trichodesmium}$ abundance was described for the first time over the total water column in the SWTP. $FTL_{Trichodesmium}$ abundance allowed one to classify 3 groups of stations, according to its Log10 of N m^{-3}. The 1st group was composed by the stations SD1 to SD7, SD8 (but not SD9) and included both LDA in the western MA and LDB in the FI (log10 >2.7). The 2nd group was composed by SD8 to SD12 with medium concentrations (2<log10 < 2.7). Finally, the 3rd group contained the stations SD13, SD14, LDC and SD15 characterized by no or very low $FTL_{Trichodesmium}$ abundance (log10 < 1).

3.2.2 Picoplankton abundance and influence on TChla biomass

Picoplankton predominance was typical of oligotrophic waters (Neveux et al., 1999; Buitenhuis et al., 2012; Bock et al., this issue). The Syn abundance was particularly high in the surface layer in the MA at SD3-LDA (> 22 10^3 cells mL^{-1}) until the intermediate area of the Fijian basin (FI), except the surface maximum at LDB (> 100 10^3 cells.mL^{-1}). The Proc abundance peaked at LDB with more than 9.10^5 cells mL^{-1} in the upper surface layer and the Peuk was high at the DCM only.

3.2.3 Chla, PE and accessory pigments

HPLC pigment analyses revealed the occurrence of three major pigments identified as

© Author(s) 2018. CC BY 4.0 License.

diverse Chla, zeaxanthin and β-carotene, classically observed in marine cyanobacteria (Higgins et al., 2011). Pigment concentrations from LOV were used as they are available for each station and depth at Fig. 4a-c (HPLC LOV laboratory data, OUTPACE data basis, J. Ras). The 0-150 m section of zeaxanthin, the main photoprotectant carotenoid contained in all cyanobacteria (Syn, Proc + *Trichodesmium*), showed an extremely rich surface layer (> 0.15 mg m^{-3}) from 0 to 50 m and almost continuously from SDA to SD12. A strong maximum was observed at the frontal LDB (Fig. 4b). TChla section (Fig. 4c) showed high values in the MA near the islands of New Caledonia-Vanuatu (SD1 to SD6) (with a maximum of 0.352 mg m^{-3} at SD1 at 5 m), and a DCM oscillating between 70 and 110 m (Table 1), with a TChla (0.534 mg m^{-3}) and an extremely shallow DCM (52 m) at the frontal LDB. Surface PE > 10 µm values (indicative of *Trichodesmium*) showed two spots of high concentrations (Fig. 4e). The first spot is located in the Western part of the MA (SD1 to SD5), and the second is located at LDB. PE was low in the central part of the transect (between SD6 and SD12), and was near 0 in the SPG. Higher surface values of TChla and PE>10 at LDA and LDB (Fig. 4d, e) are from pump samples, and provided higher values than surface Niskin samples.

DV-Chla of Proc (Fig. 5a) increased from West to East and showed a prominent maximum of 0.18 mg m^{-3} from 0 to 30 m at the frontal LDB with proportions, of 22% in the MA, 39% in the FI, and up to 39% in the SPG (and 45% at LDB). The decomposition of MV-Chla (paragraph 2.6) showed (Fig. 5a) that Syn+Peuk were not important contributors to MV-Chla biomass (< 0.011 mg.m^{-3} on average) nor the sum of nano- + micro-plankton (< 0.028 mg m^{-3}). Tricho-Chla was then between 0.15 mg m^{-3} in the MA, 0.03 mg m^{-3} in the FI, with a high value of 0.08 mg m^{-3} at LDB and < 0.02 mg m^{-3} in the SPG. Its contribution to TChla (Fig. 5b) varied from 52 to 33% between MA and FI, and still 23% of TChla in the SPG (SD12-LDC). Its % contribution at LDB was lower because of a high DV-Chla. Note that identical contributions were calculated either using LOV or NASA surface pigments (TChla-LOV and TChla-NASA was highly correlated ($TChla_{LOV} = 0.86 \times TChla_{NASA}$; $r^2 = 0.93$, $p < 0.05$, $n = 15$), and $zea_{LOV} = 0.70 \times zea_{NASA}$; $r^2 = 0.78$, $p < 0.05$, $n = 15$). The contribution of *Trichodesmium* to zeaxanthin followed roughly the same pattern, except at SD1 and was somewhat higher between SD8-SD11.

3.2.4 *Trichodesmium* abundance

The trichome concentration (L^{-1}) estimated from PE > 10 µm (paragraph 2.6) ranged from 0 in LDC SD14-15 to 4580 trich L^{-1} at SD1 (Fig. 6). The one estimated from Chla (or Chla.Trich) ranged (Fig. 6) between 3692 trich L^{-1} at SD1, 144 at SD13 and 1379 trich L^{-1} at

© Author(s) 2018. CC BY 4.0 License.

LDB. The difference between the estimation from PE >10µm or Chla at SD1 may be due to patchiness leading to a high variability of colony abundance in water samples (Fig. 6). Trichome concentration estimates from pigments showed the same pattern that the one obtained from visual counts (Fig. 6).

Fig. 7a shows significant regressions between trichome concentrations estimated from PE > 10 µm or Chla.Trich and $FTL_{Trichodesmium}$ abundance. The relatively high slopes of the correlation (900 and 600 as the factor between colonies and trichomes, from PE and Chla respectively) indicate aggregation processes. The correlation (Fig. 7b) between Chla-Tri and our visual counts (r^2=0.80) was also significant.

3.3 Absorption and backscattering coefficients, photoprotection index

Trichodesmium-rich backscattering coefficient (bb-H6) was higher by a factor of 2 at the stations with the highest *Trichodesmium* concentrations (SD1 and SD2) compared to those with lower *Trichodesmium* concentrations (SD2 to SD6) and an oceanic station off New Caledonia (Fig. 8a). It showed large troughs due to absorption maxima at these wavelengths in the blue channel (Fig. 6a-d). The section from 0 to 150 m of b_b-H6 showed that the high backscattering layer characterizes the 0-10 m in the MA (no data were collected after SD5).

Typical spectra of particulate absorption for *Trichodesmium*-rich waters (SD1, SD2, and other stations of the highest $FTL_{Trichodesmium}$ abundance group) exhibit the 2 MAAs absorption peaks at 330 and 360 nm (Fig. 9a). These peaks are visible on *in vivo* spectra (Dupouy et al., 2008) and their amplitude though enhanced by freezing (Laurion et al., 2009) are used in many studies to show the degree of photoprotection by MAAs against UV (Ferreira et al., 2013). These peaks never appear at the surface in low *Trichodesmium* concentrations (the medium $FTL_{Trichodesmium}$ abundance group; Fig 9b). Sections from 0 to 150 m of $a_P(330)$ and $a_P(440)$ (Fig. 9c, upper and lower panels) exhibit the impact of MAAs in the upper layer at 350 nm, ant the effect of the DCM at 442 nm. High values (> 80) of $a_P(330)$ (0.4 m^{-1}) and of the $a_P(330)/a_P(676)$ ratio were measured from 0 to 25 m, and abruptly felt to 20 below 30-m depth (Fig. 10a). A reasonable relationship was found between UVP-5 $FTL_{Trichodesmium}$ abundance and $a_P(330)$ when considering all depths (from 0 to 150 m) ($FTL_{Trichodesmium}$ abundance = 0.43 $a_p(330)$ -2.1, r^2 = 0.57, n = 100) (Fig. 10b). At the surface (Fig 10c), the MAAs index was variable along the transect, and was not tightly related to *Trichodesmium*. Discrepancies are seen in some stations such as SD6 and SD10 (with high values of the MAAs index and low *Trichodesmium* abundance), as at these stations,

© Author(s) 2018. CC BY 4.0 License.

phytoplanktonic cells other than *Trichodesmium* might also be protected. Indeed, MAA pigments are produced by all phytoplankton groups (Carreto and Carignan, 2011) when exposed to high $nL_w(UV)$ values. Their MAA's index might also be influenced by the value of $a_P(676)$ because of different package effect at this wavelength linked to the size. MAA's of other groups show generally only one peak at 320 nm as in the South Eastern Pacific at BIOSOPE (Bricaud et al., 2010) or at 330 nm (large phytoplankton in the Argentina continental shelf; Ferreira et al., 2003). These other groups were in low abundance at the surface at OUTPACE (as shown by the size index from HPLC).

3.4 Relationships between AOPs and pigments

In the present study, Chla was well correlated to all $nL_w(\lambda)$ ratios $[nL_w(\lambda)/nL_w(565)]$ with r^2 varying from 0.79 to 0.83 (Fig. 11). The relationships between and Chla showed the same fits as for BIOSOPE (except at 305 and 325 nm). These good relationships obtained even in the UV domain (where Chla does not absorb) were already observed in the South East Pacific, for equivalent ranges, and attributed to the fact that CDM substances covary with Chla (Tedetti et al., 2010).

3.5 Potential influence of *Trichodesmium* on the distribution of $nL_w(\lambda)$

To better assess the influence of *Trichodesmium* on the distribution of $nL_w(\lambda)$ values, the 8 radiances of the South West Pacific OUTPACE cruise (this study) and of the South East Pacific data (BIOSOPE cruise, 2004) were statistically analyzed. Fig. 12a-d represents the results of a principal component analysis (PCA) operated separately on $nL_w(\lambda)$ values and TChla concentrations for the two cruises. In the South West Pacific, the two principal components (PCs) represent 93% of total variance (Fig. 12b). The graph of correlations between PCs and the variables (Fig. 12a) indicates that UV and visible $nL_w(\lambda)$ are distributed along the PC1 axis, with all radiances on the right side, except 565 nm. This 1st axis (83% of total variance) indicates an effect of Chla on $nL_w(\lambda)$, with all $nL_w(\lambda)$ being higher at low Chla (blue waters) and lower at high Chla (mesotrophic waters), except at 565 nm, where on the contrary nL_w increases with Chla. Oligotrophic stations are on the right side and mesotrophic stations on the left. PC2 represents 9.4% of the total variance. The variables that have significant correlation with PC2 are $nL_w(565)$, (Chla rich waters) and $nL_w(490)$ (Chla poor waters), both on the upper side of the PC2 axis. A series of stations is positively linked to this PC2 axis (LDB4, SD1, SD2, LDA-2, SD7) while LDA-3 and LDA-4 are negatively linked to

© Author(s) 2018. CC BY 4.0 License.

PC2. The relatively high correlation between PC2 and $nL_w(565)$, minimally influenced by Chla, suggests that other parameters than abundance (e.g., size, type) might affect $nL_w(565)$ at the stations with sizeable PC2 values.

In comparison, the first 2 PCs for the South East Pacific dataset represent 95% of the total variance, with 89% for PC1 and only 5% for PC2 (Fig. 12c). The main difference is that $nL_w(565)$ is no more linked with PC2 but only to PC1, and that for PC2 $nL_w(490)$ has an opposite behavior compared to that in the South West Pacific (correlation is negative instead of positive). At 490 nm, Chla appears to explain most of the nL_w variability. This could reflect the absence of *Trichodesmium* in the Eastern Pacific. Except for a few stations, the PC2 contribution is much lower, i.e., variability is mostly described by PC1.

4. Discussion

4.1 Determination of the contribution of other phytoplankton and filamentous cyanobacteria to absorption and backscattering coefficients

The determination of *Trichodesmium's* influence on IOPs compared to other microorganisms and non-living particles in the sea is a main challenge. Indeed, previous models showed that absorption is governed by size and intracellular content (Bricaud et al. 1995; 2004; 2010) while backscattering is rather influenced by small particles (< 0.5 µm) of mineral origin, bubbles and colloids than by soft marine living particles (Loisel et al., 2007; Stramski et al., 2008). In oligotrophic waters of the South East Pacific, backscattering was well related to Chla (Huot et al., 2008), and recent studies in the open ocean indicate a strong correlation with particles (Dall'Olmo et al., 20109; Brewin et al., 2012; Martinez Vincente et al., 2013; Slade and Boss, 2017). Our H6-backscaterring data at OUTPACE compared to the ones of Diapalis (not shown) show that backscattering is enhanced in the presence of *Trichodesmium*. The layer of the highest backscattering coefficient is situated above the 10m-$FTL_{Trichodesmium}$ and the relationship between the vertical distribution of b_{bp}, and the vertical structure of colonies, detritus and organisms must be explored further. There is a strong link between particulate backscattering and particulate organic carbon (Stramski et al., 2008; Evers-King et al., 2017). The organic carbon content of *Trichodesmium* filaments was not estimated in the South West Pacific as trichomes counts are not yet available at all depths and stations (Dupouy et al., in prep.). However, we found total algal carbon portions were in the range 10-50% with a maximum of 75% during the bloom in the Loyalty Channel (Tenorio et

© Author(s) 2018. CC BY 4.0 License.

al., in press). Additional work is needed to model influence of *Trichodesmium* in terms of pigment biomass, and carbon biomass on $nL_w(\lambda)$ values.

4.2 Specificity of fluorescence and pigmentation of *Trichodesmium* for interpreting satellite Chla imagery

Is has been shown that in the upper layer of the 0-150m section, particularly in the western part of the MA, that highest *Trichodesmium* abundance and $a_P(330)$ are well correlated. At the opposite, $a_P(440)$ is lower than expected for this *Trichodesmium* abundance. *Trichodesmium*-specific Chla values retrieved from satellite observations, are expected to be 4 times lower because of a shadow effect on absorption of light by colony (until a factor of 4 (Subramanian et al., 1999; McKinna, 2015). It was also noted that the CTD fluorescence signal was also weak as already noted in the region (Diapalis; Tenorio et al., in press). Last, it can be attributed to a "deficient" response of large colonies to the laser compared with the numerous small picoplanktonic cells (Neveux et al., 2010). This can be attributed to a "deficient" response of large colonies to the laser compared with the numerous small picoplanktonic cells (Neveux et al., 2010). Note that Chla should be measured also on a sufficient volume to catch colonies, adjusted as a to expected abundance.

4.3 The influence of *Trichodesmium*-CDOM to ocean color

High CDM amount is expected to be associated *Trichodesmium*, either from CDOM issued from degradation of colonies, and/or from MAAs absorption (Subramaniam et al., 1999a; Steinberg et al., 2004; Dupouy et al., 2008). MAAs identified by their strong UV absorption at 332 and 362 nm are the water-soluble pigments asterina-330 and shinorine as the most abundant, and the mycosporine-like amino acids, like glycine and porphyra-334, and palythene-360 as minor components. In order to define the best photoprotection index for *Trichodesmium*, it would be useful to take into account the double absorption peak at 330 and 360 nm and variability of absorption peak at 676nm as a function of size (Bricaud et al., 2010). Indeed, a complete analysis of the different components of CDM measured during the cruise over the whole water column has still to be achieved.

4.4. Contribution of *Trichodesmium* spp. to TChla and ocean color

All *Trichodesmium* abundance data, obtained from UVP5, pigments and flow cytometry data, or from visual counts showed a high abundance in the MA that strongly

© Author(s) 2018. CC BY 4.0 License.

529 influences the Chla biomass in the western part of the Melanesian archipelago and a lower
530 abundance in the SPG, with a mean value at LDB. Trichome abundance estimated from the
531 decomposition of pigments were equivalent to the ones enumerated with the microscopy in
532 the region (at 167°E, 21°S, Diapalis data; Shiosaki et al., 2014). The UVP5 counted the
533 largest colonies of the *Trichodesmium* population, i.e. the upper part of the colony size
534 distribution. The factor between these counts and estimated trichome concentrations (1000)
535 depends on the number of isolated or small colonies (unknown) and from other aggregation
536 processes which remain to analyse further. From literature data, this number varies between
537 200 for the highest to 50 for the lowest (Davis and McGillicudy, 2006; Guidi et al., 2012;
538 Olson et al. 2015) and the largest numbers found here may indicate different proportions in
539 colonies and trichomes in the South Western tropical Pacific. High colony abundance was
540 detected from 0 to 30 meters with the UVP5 even though colonies are detected deeper with
541 this instrument. Their abundance was low. In the region, trichomes are generally found from
542 0 to 60 meters (Tenorio et al., in press). The high contribution of *Trichodesmium* detected
543 during OUTPACE in the Western part of the Melanesian archipelago (around New Caledonia
544 and Vanuatu) between 158 and 174°E and at the frontal accumulation at 170°W match the
545 large amount of surface mats detected from the satellite in this part of the transect (Dupouy et
546 al., 1988; 2000; 2011) and was observed during the OUTPACE cruise thanks to a new
547 algorithm developed for the region (Rousset et al., this issue). It is the first time that this
548 continuity of *Trichodesmium* is measured with a profiler from 0 to 150 meters on the whole
549 Southwest tropical Pacific. Even if *Trichodesmium* abundance is lower around 180, there
550 might be enough colonies below the surface (less visible by the satellite) to produce mats, as
551 soon as environmental conditions are favourable (as there are observed there, but more
552 episodically) than at 170°E where they are frequent.

553 Proc was the other dominant group impacting the Chla biomass. Two parts of the
554 SWTP ocean at 174°E (SD7): (1) the western part of the MA between New Caledonia and
555 Vanuatu, impacted by a large contribution by *Trichodesmium* and (2) the eastern part of the
556 transect (FI), more oligotrophic and impacted by *Prochlorococcus* and other picoplanktonic
557 groups. LDB was the only exception showing a high abundance of both *Trichodesmium* and
558 other groups, with TChla proportions of *Trichodesmium*, Syn+Peuk, Micro, Nanoeuk, and
559 Proc of 25, 7, 1.4, 5 and 45 %, respectively.

560 OUTPACE and BIOSOPE radiometric data show that the South West and South East
561 Pacific surface waters exhibited similar ranges of values for $nL_w(\lambda)$ and Chla (0-0.58 and

© Author(s) 2018. CC BY 4.0 License.

562 0.02-1.3 mg m^{-3}, respectively). It should be noticed that this "extreme" value of 1.3 mg m^{-3}
563 was recorded in the Peru upwelling. OUTPACE and BIOSOPE data differed in only two
564 spectral bands. OUTPACE and BIOSOPE radiance data with the OCR UV-Vis radiometer
565 differed in only two spectral bands. The PC1 axis was linked to Chla concentration for both
566 cruises. PC2 was linked to another optically active variable, independent of Chla. For
567 OUTPACE, the different behaviors in $nL_w(565)$ (yellow) and $nL_w(490$ nm) (green) are
568 significant compared to the sensitivity of the instrument. The significance of PC2 (linked to
569 an increase of $nL_w(565)$ for Chla rich waters) is clear. It is absent in the South East Pacific
570 meaning that all these processes were not occurring during the BIOSOPE cruise, i.e. there is
571 no effect of particles or PE at high Chla concentrations. Indeed, Huot et al. (2008) showed
572 that backscattering measured during the BIOSOPE stations (between 41°W and 173°W) is
573 totally linked to Chla.

574 The relationship of $nL_w(490)$ to PC2 is more difficult to interpret due to its opposite
575 behavior between the South West and the South East Pacific. PCA shows that the variability
576 in $nL_w(490$, green) and $nL_w(565$, yellow) is not totally determined by Chla, as it exists a non-
577 negligible correlation between PC2 and these green and yellow radiances. However this effect
578 is reversed between these two areas. One explanation would be that in the presence of
579 *Trichodesmium*, it is expected a higher backscattering (linked to another factor than Chla) and
580 a PE fluorescence in the yellow, but also a high backscattering in the green. However, in the
581 green, there is a possible effect of the absorption by zeaxanthin (the major photoprotecting
582 pigment, not totally correlated with Chla as shown by the PCA). PCA applied to the only nLw
583 and Chla variables does not allow one to explain the correlation between PC2 and $nL_w(490)$
584 (due to a different pigment, PE fluorescence or backscattering). At BIOSOPE, where
585 $nL_w(490)$ is essentially function of Chla, the zeaxanthin effect would be negligible or totally
586 linked with the one of Chla.

587 The spectrum obtained from an optical model of a *Trichodesmium's* bloom at 0.5 mg
588 Chla m^{-3} showed a similar shape than those from other phytoplankton, but with higher
589 magnitudes for $nL_w(490)$, $nL_w(510)$ and $nL_w(555)$ (Subramaniam et al., 2002). At 0.5 mg
590 Chla m^{-3}, the magnitude of $nL_w(510)$ was greater than $nL_w(443)$, and for middle
591 concentrations, from 0.5 and 1.5 mg Chla m^{-3}, the model predicted that a peak should be
592 observed at $nL_w(490)$. At concentrations approximating 2 mg Chla m^{-3} and higher, $nL_w(555)$
593 exceeded $nL_w(490)$. These two wavelengths were those chosen by Westberry and Siegel
594 (2006) to set an algorithm to map *Trichodesmium* globally with SeaWiFS. Nevertheless, the

© Author(s) 2018. CC BY 4.0 License.

595 results were not satisfactory around SWTP islands, even in summer when blooms are
596 numerous (Dupouy et al., 2011). The reason why their algorithm was not successful around
597 New Caledonia might be due to an inappropriate radiance model at 490nm and 565 nm in the
598 case of moderate *Trichodesmium* abundance.
599

600 ## 5 Conclusions

601 The OUTPACE cruise in the South West Tropical Pacific from 158°E to 160°W
602 provided a unique set of simultaneous measurements of $nL_w(\lambda)$ in the ultraviolet and visible
603 domains, pigments, and *Trichodesmium* and picoplanktonic cell abundance along the whole
604 transect during a summer bloom. *Trichodesmium* abundance given by the UVP5 (i.e., largest
605 colonies) was well correlated with the trichome concentration estimated at the surface from
606 pigment algorithms and visual counts. The factor of 600-900 observed between large colonies
607 and trichome concentration is indicative of aggregation processes, and is also specific to all
608 cameras towered or lowered in the ocean. *Trichodesmium* abundance was also well correlated
609 with the absorption peak of MAA's, i.e. $a_P(330)$ and the photoprotection index. This
610 demonstrates that UVP5 is a well adapted instrument for exploring the variability of
611 *Trichodesmium* in the water column, and that $a_P(330)$ or photoprotection index, is a useful
612 parameter to quantify the latter. The weak CTD-fluorescence and blue absorption observed in
613 rich-*Trichodesmium* waters tend to underestimate *Trichodesmium* abundance if used on
614 profilers while the backscattering (high coefficient, spectral troughs) tend to correctly
615 estimate *in situ* aggregations. Along the 165°E-170°W transect, *Trichodesmium* together with
616 *Prochlorococcus* represented the major part of TChla (the other groups were negligible).
617 *Trichodesmium* contribution to TChla was the highest in the Western part of the Melanesian
618 Archipelago (around New Caledonia and Vanuatu), regularly decreased to the East, in the
619 vicinity of the Fiji Islands, reaching a minimum in the South Pacific gyre stations where the
620 *Prochlorococcus* contribution to TChla was higher. It is the first time that this continuity from
621 0 to 150 m of *Trichodesmium* abundance is measured with a profiler on the whole South West
622 tropical Pacific. Then, even if *Trichodesmium* abundance is lower south of Fijian Islands,
623 there might be enough colonies below the surface (less visible by the satellite) to produce
624 mats, as soon as the environment is favourable (as it is observed, but more episodically than at
625 170°E).

626 During OUTPACE, the relationship between normalized water radiance, nL_w, and
627 Chla was generally similar to that found in the Eastern Tropical Pacific during BIOSOPE. In

© Author(s) 2018. CC BY 4.0 License.

628 particular, radiance ratios were related to Tchla in the visible and the UV domain interpreted
629 as a strong coupling between the UV-absorbing Chromophoric Dissolved Material and Chla.
630 Principal component analysis (PCA) of OUTPACE data showed that nL_w in the ultraviolet
631 and visible were strongly correlated to Chla except in the green and yellow (490 and 565
632 nm). These results, as well as differences in the PCA of BIOSOPE data, suggested that
633 that nL_w variability in the green and yellow radiance during OUTPACE was influenced by
634 other variables associated with *Trichodesmium* presence, namely a specific backscattering
635 coefficient, phycoerythrin fluorescence, and/or zeaxanthin absorption. These green (490 nm)
636 and yellow (565 nm) wavelengths are often chosen in *Trichodesmium* detection algorithms.
637 Indeed, more work is required to explain the PCA results. It would be useful to include
638 backscattering coefficient, PE, photoprotecting carotenoids from HPLC and *Trichodesmium*
639 abundance at all depths into the PCA analysis. Also, it would be useful to compare our
640 measured radiance in this *Trichodesmium* bloom to modeled radiance of classical
641 phytoplankton to highlight potential anomalies, and last, to decompose the effect of
642 *Trichodesmium* specific IOPs and pigments on radiance. While detecting *Trichodesmium* mats
643 with the "red edge" is essential (Rousset et al., this issue), as this part of colonies may also
644 actively fix N2, exploring the green-yellow change in ocean color detected here at regular
645 *Trichodesmium* concentrations is probably the only way to assess true nitrogen fixation rates
646 in the SWTP.

647 ***Acknowledgments.*** The authors thank the crew of the R/V L'Atalante from operation at sea.
648 We acknowledge Joséphine Ras, CNRS, for the OUTPACE HPLC databasis and Crystal
649 Thomas, NASA, for surface and DCM HPLC data. We thank Mireille Pujo-Pay for her
650 scientific advices on board R/V *Atalante*. We thank Benjamin Blanc for sorting and validating
651 images from the UVP-5. We acknowledge David Varillon, IRD US IMAGO, and Philippe
652 Gérard for Chla analyses and the administrative staff of Center of Noumea. Jacques Neveux
653 and Rüdiger Röttgers are acknowledged for helpful discussions during the elaboration of the
654 manuscript. This is a contribution of the OUTPACE (Oligotrophy from Ultra-oligoTrophy
655 PACific Experiment) project (https://OUTPACE.mio.univ-amu.fr/) funded by the French
656 research national agency (ANR-14-CE01-0007-01), the LEFECyBER program (CNRS-
657 INSU), the GOPS program (IRD) and the Centre National d'Etudes Spatiales (BC T23, ZBC
658 4500048836). The OUTPACE cruise (http://dx.doi.org/10.17600/15000900) was managed by
659 MIO Institute from Marseilles (France). The National Science Foundation supported SD
660 under grant OCE-1434916.

Biogeosciences Discuss., https://doi.org/10.5194/bg-2017-570
Manuscript under review for journal Biogeosciences
Discussion started: 15 January 2018
© Author(s) 2018. CC BY 4.0 License.

661

662

663 **Table 1**. Main characteristics of the OUTPACE stations.

Station	Longitude	Latitude	Date	UT time	TChl*a* (mg m^{-3})	$FTL_{Tric\ hodesmium}$ ($N.m^{-3}$)	DCM (m)	PE (mg m^{-3})	$K_d(\lambda)$ (m^{-1}) 305 nm	325 nm	340 nm	380 nm	PAR
SD1	159°54' E	18°00'S	21 Fev.15	20h00	0.352	4125	101	1.15	0.173	0.116	0.093	0.05	nd
SD2	162°07' E	18°37' S	22 Fev. 15	21h45	0.278	2430	70	0.122	0.194	0.119	0.099	0.057	0.026
SD3	164°54' E	19°00' S	24 Fev.15	03h45	0.236	445	70	0.08	nd	nd	nd	nd	0.028
LDA*	164°41' E	19°13' S	25 Fev. 15	13h00	0.220	974	100	0.10	0.074	0.041	0.029	0.012	0.024
SD4	168°00' E	20°00' S	04 Mar. 15	08h30	0.199	1674	70	0.43	nd	nd	nd	nd	nd
SD5	170°00'S	22°00' S	05 Mar. 15	05h45	0.258	902	70	0.26	nd	0.124	0.083	0.048	nd
SD6	172°08' E	21°22' S	06 Mar. 15	03h15	0.265	935	130	0.05	0.159	0.108	0.087	0.044	0.025
SD7	174°16' E	20°44' S	07 Mar. 15	00h00	0.186	1059	110	0.08	0.117	0.073	0.053	0.009	0.019
SD8	176°24' E	20°06' S	07 Mar. 15	21h00	0.138	165	120	0.03	0.143	0.087	0.065	0.026	0.021
SD9	178°39' E	20°57' S	08 Mar. 15	22h15	0.236	569	120	0.08	0.152	0.097	0.074	0.041	0.020
SD10	178°31' W	20°28' S	10 Mar. 15	00h00	0.113	127	120	0.04	0.139	0.086	0.065	0.034	0.020
SD11	175°40' W	19°59' S	10 Mar. 15	21h45	0.185	188	110	0.09	0.137	0.082	0.06	0.024	0.033
SD12	172°50' W	19°29' S	11 Mar. 15	21h00	0.133	139	120	0.04	0.116	0.069	0.051	0.027	0.020
LDB*	170°52' W	18°14' S	15 Mar. 15	23h00	0.433	2950	52	0.24	0.172	0.11	0.087	0.054	0.028
SD13	169°04' W	18°12' S	21 Mar. 15	22h30	0.0357	4	125	0.00	nd	nd	nd	nd	nd
LDC*	165°45' W	18°41' S	23 Mar. 15	01h00	0.0231	0.82	135	0.01	0.189	0.116	0.09	0.054	0.020

Biogeosciences Discuss., https://doi.org/10.5194/bg-2017-570
Manuscript under review for journal Biogeosciences
Discussion started: 15 January 2018
© Author(s) 2018. CC BY 4.0 License.

SD14	163°00' W	18°25' S	30 Mar. 15	01h30	0.045	0	165	0.04	nd	0.056	0.04	0.023	0.018
SD15	160°00' W	18°16' S	31 Mar. 15	00h00	0.061	0	110	0.00	0.097	0.054	0.039	0.021	0.016

664 TChla: average concentrations in total chlorophyll a (monovinyl Chla + divinyl Chla) in surface waters derived from HPLC
665 analyses, based on duplicate analyses (CV < 8%). FTL$_{Trichodesmium}$ abundance: determined using underwater vision profiler 5 (UVP5).
666 DCM: deep chlorophyll maximum. PE: phycoerythrin. $K_d(\lambda)$: diffuse attenuation coefficient for downward irradiance in the UV (305, 325, 340,
667 380 nm) and PAR (400-700 nm) domains.
668 * Values for Long Duration stations, i.e., LDA, LDB and LDC, averaged over 7 days.
669
670

© Author(s) 2018. CC BY 4.0 License.

671

672 REFERENCES

673 Biegala I. C., Aucan J., Desnues A., Rodier M., Dupouy C., Raimbault P., Douillet P., Hunt
674 B., Pagano M., Clavere-Graciette A., Bonnefous A., Roumagnac M., Gasol J., Periot
675 M., Schenkels O., Sharma P., Harlay J., Eldin G., Cravatte S., Marin F., Varillon D.,
676 Roubaud F., Jamet L., Gérard P., Goyaud A., Legrand H., Gouriou Y., and
677 Ganachaud A.: The South Pacific Ocean Time Series (SPOT) station : a first focus
678 on diazotrophs community, http://www.eposters.net/poster/the-south-pacific-ocean-
679 time-series-spot-station-a-first-focus-on-diazotrophs-community, 2014
680 Blondeau-Patissier, D., Gower, J. F. R., Dekker A. G., Phinn, S. R., Brando V. E.:A review
681 of ocean color remote sensing methods and statistical techniques for the detection,
682 mapping and analysis of phytoplankton blooms in coastal and open oceans - Progress
683 in oceanography, 123, 123-144, 2014
684 Bock, N., Van Wambeke, F., Dion, M. and Duhamel, S.: Microbial community structure in
685 the Western Tropical South Pacific, Biogeosciences, this issue.
686 Bonnet, S., Caffin, M., Berthelot, H., and Moutin, T.: Hot spot of N2 fixation in the western
687 tropical South Pacific pleads for a spatial decoupling between N2 fixation and
688 denitrification, PNAS letter, doi/10.1073/pnas.1619514114, 2017.
689 Borstad, G. A., Gower, J., and Carpenter, E.: Development of algorithms for remote sensing
690 of *Trichodesmium* blooms. in E.J. Carpenter et al. (eds), Marine Pelagic
691 Cyanobacteria: *Trichodesmium* and other Diazotrophs, 193-210, 1992.
692 Bracher, A., Bouman, H. A., Brewin, R. J. W., Bricaud, A., Brotas, V., Ciotti, A. M.,
693 Clementson, L., Devred, E., Di Cicco, A., Dutkiewicz, S., Hardman-Mountford, N.
694 J., Hickman, A. E., Hieronymi, M., Hirata, T., Losa, S. N., Mouw, C. B., Organelli,
695 E., Raitsos, D. E., Uitz, J., Vogt, M., and Wolanin, A.: Obtaining Phytoplankton
696 Diversity from Ocean Color: A Scientific Roadmap for Future Development, Front.
697 Mar. Sci. 4:55, 2017.
698 Brewin, R. J. W., Hardman-Mountford, N. J., Lavender, S. J., Raitsos, D. E., Hirata, T., Uitz,
699 J., et al.: An inter-comparison of bio-optical techniques for detecting dominant
700 phytoplankton size class from satellite remote sensing, Remote Sens. Environ. 115,
701 325–339, 2011.
702 Brewin, R. J. W., Dall'Olmo, G., Sathyendranath, S., and Hardman-Mountford, N. J.: Particle
703 backscattering as a function of chlorophyll and phytoplankton size structure in the
704 open-ocean, Optics Express, 20, 17632–17652, 2012.
705 Bricaud, A., Babin, M., Morel, A. and Claustre H.: Variability in the chlorophyll-specific
706 absorption coefficient of natural phytoplankton: analysis and parametrization.
707 Journal of Geophysical Research, 100, C7, 13321-13332, 1995.
708 Bricaud, A., Claustre, H., Ras, J., and Oubelkheir, K.: Natural variability of phytoplanktonic
709 absorption in oceanic waters: Influence of the size structure of algal populations,
710 Journal of Geophysical Research, 109, C11010, 2004.
711 Bricaud, A., Babin, M., Claustre, H., Ras, J., and Tièche, F.: Light absorption properties and
712 absorption budget of Southeast Pacific waters, Journal of Geophysical Research, 115,
713 C08009, 2010.
714 Capone, D.G., Zehr, J. P., Paerl, H. W., Bergman, B., and Carpenter, E. J.: *Trichodesmium*, a
715 globally significant marine cyanobacterium. Science 276, 1221.
716 Carpenter, E. J., O'Neil, J. M., Dawson, R., Capone, D. G., Siddiqui, P. J. A., Roenneberg T.
717 and Bergman B.: The tropical diazotrophic phytoplankter *Trichodesmium*: biological

© Author(s) 2018. CC BY 4.0 License.

characteristics of two common species. Marine Ecology Progress Series, 95, 3, 295-304, 1993.

Carpenter, E. J., Subramaniam, A., and Capone, D.G.: Biomass and primary productivity of the cyanobacterium *Trichodesmium* spp. in the tropical North Atlantic Ocean. Deep Sea Res., Part I, 51, 173–203, 2004.

Carreto, J.I., and Carignan, M. O.: Mycosporine-like amino acids: relevant secondary metabolites. Chemical and ecological aspects, Mar. Drugs, 9, 387–446, 2011.

Dall'Olmo, G.,. Westberry, T. K., Behrenfeld, M. J., Boss, E., and Slade, W. H.: Significant contribution of large particles to optical backscattering in the open ocean. Biogeosciences, 6, 947–967, 2009.

Dandonneau Y., and Niang, A.: Assemblages of phytoplankton pigments along a shipping line through the North Atlantic and Tropical Pacific. Progress in Oceanography, 73 (2), 127-144, 2007.

Davis, C. S., and McGillicuddy, D. J. Jr.: Transatlantic abundance of the N2-fixing colonial cyanobacterium Trichodesmium, Science, 312(5779), 1517–1520, 2006.

De Boissieu, Menkes, C., Dupouy, C., Rodier, M., Bonnet, S., and Frouin, R. : Phytoplankton global mapping from space with a Support Vector Machine algorithm, Proc. of SPIE Vol. 9261, 92611R, SPIE, 2014.

Dupouy, C., Loisel, H., Neveux, J., Brown, S. L., Moulin, C., Blanchot, J., Le Bouteiller, A., and Landry, M. R.: Microbial absorption and backscattering coefficients from in situ and POLDER satellite data during an El Nino–Southern Oscillation cold phase in the equatorial Pacific (180°), Journal of Geophysical Research, 108(C12), 8138, 2003.

Dupouy, C., Neveux, J., Dirberg, G., Röttgers, R., Tenório, M. M. B., and Ouillon, S.: Bio-optical properties of the marine cyanobacteria *Trichodesmium* spp, J. Appl. Remote Sens., 2, 1–17, 2008.

Dupouy, C., Petit, M., and Dandonneau, Y.: Satellite detected cyanobacteria bloom in the southwestern tropical Pacific. Implication for nitrogen fixation, International Journal of Remote Sens., 8, 389–396, 1988.

Dupouy C., Neveux J., Ouillon S., Frouin, R., Murakami H., Hochard S., and Dirberg, G.: Inherent optical properties and satellite retrieval of chlorophyll concentration in the lagoon and open ocean waters of New Caledonia, Mar. Pollut. Bull., 61, 503–518, 2010.

Dupouy, C., Benielli-Gary, D., Neveux, J., Dandonneau, Y. and Westberry, T.K..: An algorithm for detecting Trichodesmium surface bloom in the South Western Tropical Pacific, Biogeosciences, 8, 3631–3647, 2011.

Evers-King, H., Martinez-Vicente, V., Brewin, R. J., Dall'Olmo, G., Hickman, A. E., Jackson, T., Kostadinov, T. S., Krasemann, H., Loisel, H., Röttgers, R., Roy, S., Stramski, D., Thomalla, S., Platt, T., and Sathyendranath, S.: Validation and intercomparison of ocean color algorithms for estimating particulate organic carbon in the oceans, Front. Mar. Sci. 4:251. 10.3389/fmars.2017.00251, 2017.

Ferreira, A., D. Stramski, C. A. E. Garcia, V. M. T. Garcia, A. M., Ciotti, and Mendes, C.R.B.: Variability in light absorption and scattering of phytoplankton in Patagonian waters: Role of community size structure and pigment composition, J. Geophys. Res. Oceans, 118, 698–714, 2013.

Gordon, H. R. Normalized water-leaving radiance: Revisiting the influence of surface roughness, Appl. Opt., 44, 241 – 248, doi:10.1364/ AO.44.000241, 2005

Gower, J., King, S., and Young, E.: Global remote sensing of *Trichodesmium*. International Journal of Remote Sensing 35, 5459-5466, 2014.

Grob, C., O. Ulloa, O., H. Claustre, H., Y. Huot, Y., G. Alarcón, G. et al.. Contribution of

© Author(s) 2018. CC BY 4.0 License.

picoplankton to the total particulate organic carbon concentration in the eastern South Pacific. Biogeosciences, 4 (5), pp.837-852, 2017.

Guidi, L., Calil, P. H. R., Duhamel, S., Björkman, K. M., Doney, S. C., Jackson, G. A., Li, B., Church, M. J., Tozzi, S., Kolber, Z. S., Richards, K.J., Fong, A. A., Letelier, R. M., Gorsky, G., Stemmann, L., and Karl, D. M.: Does eddy-eddy interaction control surface phytoplankton distribution and carbon export in the North Pacific Subtropical Gyre ? J. Geoph. Res., 117, G02024, doi:10.1029/2012JG001984, 2012.

Higgins, H. W., Wright, S. W., and Schluter, L.: Quantitative Interpretation of Chemotaxonomic Pigment Data, Chapter 6, Phytoplankton Pigments: Characterization, Chemotaxonomy and Applications in Oceanography, Suzanne Roy, Einar Skarstad Egeland, Geir Johnsen and Carole Anne Llewellyn (eds.) Cambridge University Press, 2011.

Hooker, S. B., L. Clementson, C. S. Thomas, et al.: The Fifth SeaWiFS HPLC Analysis Round-Robin Experiment (SeaHARRE-5). NASA Technical Memo. 2012-217503 NASA Goddard Space Flight Center, Greenbelt, Maryland, 98, 2012.

Hu, C., Cannizzaro, J., Carder, K. L., Muller-Karger, F. E., and Hardy, R.: Remote detection of *Trichodesmium* blooms in optically complex coastal waters: Examples with MODIS full-spectral data. Remote Sensing of Env., 114(9): 2048–2058, 2010.

Huot, Y., Morel, A., Twardowski, M. S., Stramski, D., and Reynolds, R. A.: Particle optical backscattering along a chlorophyll gradient in the upper layer of the eastern South Pacific Ocean, Biogeosciences, 5, 495–507, 2008

Kirk, T.O.: Light and Photosynthesis in Aquatic Ecosystems, Cambridge University Press, Nature - 509 pp, 1994

Lantoine, F, and Neveux, J.: Spatial and seasonal variations in abundance and spectral characteristics of phycoerythrins in the Tropical Northeastern Atlantic Ocean. Deep-Sea Res I 44 (2): 223-246, 1997.

Laurion, I., and Roy, S.: Growth and photoprotection of natural and enhanced ultraviolet-B radiation, rowth and photoprotection in three dinoflagellates (including two strains of *Alexandrium Tamarense*) and one diatom exposed to four weeks of natural and enhanced ultraviolet-N radiation. Journal of Phycology, 45, 1, 16–33, 2009.

Laviale, M., and Neveux, J.: Relationships between pigment ratios and growth irradiance in 11 marine phytoplankton species, MEPS 425:63-77, 2011.

Loisel H., Meriaux, X., Berthon, J. F., and Poteau, A.: Investigation of the optical backscattering to scattering ratio of marine particles in relation to their biogeochemical composition in the eastern English Channel and southern North Sea, Limnol. Oceanogr., 2, 739-752, 2007.

Le Bouteiller, A., Blanchot, J., and Rodier, M.: Size distribution patterns of phytoplankton in the western Pacific: towards a generalization for the tropical open ocean, Deep Sea Res. Part A. Oceanogr. Res. Pap., 39, 805–823, 1992.

Martinez-Vicente, V; Dall'Olmo, G, Tarran, GA, Boss, EB, and Sathyendranath, S.: Optical backscattering is correlated with phytoplankton carbon across the Atlantic Ocean. Geophysical Research Letters, 40. 1-5, 2013.

McKinna, L. I. W., Furnas, M. J., and Ridd, P. V.: A simple, binary classification algorithm for the detection of Trichodesmium spp. within the Great Barrier Reef using MODIS imagery, Limnol. Oceanogr. Methods, 9, 50–66, 2011.

McKinna, L. I. W.: Three decades of ocean-color remote-sensing *Trichodesmium* spp. in the World's oceans: a review, Progress in Oceanography, 131, 177-199, 2015

Mobley, C. D.: Light and Water: Radiative Transfer in Natural Waters, Academic Press, San Diego, Calif., 1994

© Author(s) 2018. CC BY 4.0 License.

Morel A., and Maritorena, S.: Bio-optical properties of oceanic waters: A reappraisal. Journal of Geophysical Research, 106, 7163–7180, 2001.

Morel A., Gentili, B., Claustre, H., Babin, M., Bricaud, A., Ras, J., and Tieche, F.: Optical properties of the ''clearest'' natural waters, Limnol. Oceanogr., 52(1), 217-229, 2007.

Moutin, T., Doglioli, A. M., de Verneil, A., and Bonnet, S.: Preface: The Oligotrophy to the UlTra-oligotrophy PACific Experiment (OUTPACE cruise, 18 February to 3 April 2015), Biogeosciences, 14, 3207–3220, 2017.

Neveux, J., Lantoine, F., Vaulot, D., Marie, D., and Blanchot, J.: Phycoerythrins in the southern tropical and equatorial Pacific Ocean: evidence for new cyanobacterial types, Journal of Geophysical Research, 104, 3311-3321, 1999.

Neveux, J., Tenorio, M. M. B., Dupouy, C., and Villareal, T.: Spectral diversity of phycoerythrins and diazotrophs abundance in tropical South Pacific, Limnol. Oceanogr., 51, 4, 1689–1698, 2006.

Neveux, J., Lefebvre, J-P, Le Gendre R., Dupouy, C., Gallois F., Courties C., Gérard P., Ouillon, S., and Fernandez, J.M. : Phytoplankton dynamics in New-Caledonian lagoon during a southeast trade winds event. Journal of Marine Systems, 82(4), 230-244, 2010.

Olson, E. M McGillicuddy, D. J. Dyhrman, S. T. Waterbury, J. B., Davis, C. S., and Solow, A. R.: The depth-distribution of nitrogen fixation by *Trichodesmium* spp. colonies in the tropical–subtropical North Atlantic, Deep Sea Research Part I: Oceanographic Research Papers, 104, 72-91, 2015.

Picheral, M., Guidi, L., Stemmann L., Karl, D. M., Iddaoud G. and Gorsky, G. : The Underwater Vision Profiler 5: An advanced instrument for high spatial resolution studies of particle size spectra and zooplankton, Limnol. Oceanogr.: Methods, 8, 2010, 462–473, 2010.

Ras J., Uitz, J., and Claustre, H.: Spatial variability of phytoplankton pigment distributions in the Subtropical South Pacific Ocean: comparison between in situ and modelled data. Biogeosciences, 5, 353-369, 2008.

Rousselet, L., de Verneil, A., Doglioli, A. M., Petrenko, A. A., Duhamel, S., Maes, C., and Blanke, B.: Large to submesoscale surface circulation and its implications on biogeochemical/biological horizontal distributions during the OUTPACE cruise (SouthWest Pacific), Biogeosciences Discuss., 1-29, doi.org/10.5194/bg-2017-456,

Rousset, G., De Boissieu, F., Lefèvre, J., Rodier, M., Laran, S., Ridoux V., Roudault G., Gardes, L., Frouin, R., Menkes, C., and Dupouy, C.: Remote Sensing of *Trichodesmium* spp. mats in the open ocean of the Southwestern Tropical Pacific. Biogeoscience, this issue

Sempéré, R., Para, J., Tedetti, M., Charrière, B., and Mallet, M.: Variability of Solar Radiation and CDOM in Surface Coastal Waters of the Northwestern Mediterranean Seat al., Photochemistry and Photobiology, 2015, 91: 851–861, 2015.

Slade, W. H. and Boss, E.: Spectral attenuation and backscattering as indicators of average particle size, Appl. Opt. 54, 7264-7277, 2015.

Shiozaki, T., Kodama, T., and Furuya, K.: Large-scale impact of the island mass effect through nitrogen fixation in the western South Pacific Ocean, Geophys. Res. Lett., 41, 2907-2913, 2014.

Subramaniam, A., Carpenter, E. J., Karentz, D., and Falkowski, P. G.: Bio-optical properties of the marine diazotrophic cyanobacteria *Trichodesmium* spp. I- Absorption and photosynthetic action spectra, Limnol. Oceanogr., 44, 608–617, 1999a.

Subramaniam, A., Carpenter, E.J., and Falkowski, P.G.: Optical properties of the marine

© Author(s) 2018. CC BY 4.0 License.

diazotrophic cyanobacteria *Trichodesmium* spp. II- A reflectance model for remote-sensing. Limnol. and Oceanogr. 44, 618–627, 1999b.

Subramaniam, A., Brown, C. W., Hood, R. R., Carpenter, E. J., and Capone, D. G.: Detecting *Trichodesmium* blooms in SeaWiFS imagery, Deep-Sea Res. Part I, 49, 107-121, 2002.

Stramski, D., Reynolds, R. A., Babin, M., Kaczmarek, S., Lewis, M. R., et al.: Relationships between the surface concentration of particulate organic carbon and optical properties in the eastern South Pacific and eastern Atlantic Oceans. Biogeosciences, 5 (1), 171-201, 2008.

Tedetti, M., Sempéré, R., Vasilkov, A., Charrière, B., Nérini, D., Miller, W., Kawamura, K., and Raimbault, P.: High penetration of ultraviolet radiation in the south east Pacific waters, Geophys. Res. Lett., 34, L12610, doi:10.1029/2007 GL029823, 2007.

Tedetti, M., Charrière, B., Bricaud, A., Para, J., Raimbault, P., and Sempéré, R.: Distribution of normalized waterleaving radiances at UV and visible wave bands in relation with chlorophyll a and colored detrital matter content in the southeast Pacific, Journal of Geophysical Research, 115, C02010, 2010.

Tenorio, M., Dupouy, C., Rodier, M., Neveux, J.: Trichodesmium and other Filamentous Cyanobacteria in New Caledonian waters (South West Tropical Pacific) during an El Niño Episode, Aquatic Microbial Ecology, in press.

Uitz, J., Claustre, H., Morel, A., and Hooker, S. B.: Vertical distribution of phytoplankton communities in open ocean: An assessment based on surface chlorophyll, Journal of Geophysical Research, 111, C08005, doi:10.1029/2005JC003207, 2006.

Westberry, T., Subramaniam, A., and Siegel, D.: An improved bio-optical algorithm for the remote sensing of *Trichodesmium* spp. blooms, Journal of Geophysical Research, 110, C06012, 2005.

Westberry, T. K. and Siegel, D. A.: Spatial and temporal distribution of *Trichodesmium* blooms in the world's oceans, Global Biogeochem. Cy., 20, 4016, 2006.

Wyman, M.: An in vivo method for the estimation of phycoerythrin concentrations in marine cyanobacteria (*Synechococcus* spp.), Limnol. Oceanogr., 37, 1300–1306, 1992.

FIGURE LEGENDS

Figure 1. Chlorophyll composite from MODIS on the period of the OUTPACE cruise. The positions of the short (long) duration stations are shown by cross (plus) symbols. The ocean color satellite products are produced by CLS. New Caledonia, Vanuatu and Fiji islands at 165°, 170°E, and 180°E. Tonga Trench at 170°W (190°E).

Figure 2. OUTPACE AOPs: a) Box-and-whisker plots for the distribution of $nL_w(\lambda)$ in the UV (305, 325, 340, and 380 nm) and visible (412, 443, 490, and 565 nm) spectral domains determined between 0^- and 30 m in the Western tropical South Pacific at stations in the Melanesian arch. (MA, SD1-SD7 and LDA), Fijian arch. (FI, SD8-SD11), and South Pacific Gyre (SPG, SD13, LDC, SD14, SD15). The outliers stations are indicated on the upper left (see text). b) $nL_w(\lambda)$ *versus* wavelength with a color-code depending on TChla (in red: high concentrations, in black: median concentrations, in blue oligotrophic.

Figure 3. OUTPACE AOPs (continued). $Z_{10\%}(\lambda)$ at 305 nm (UV-B), and 325, 340 and 380 nm (UVA-A) at all stations during OUTPACE in the Western tropical South Pacific with a

© Author(s) 2018. CC BY 4.0 License.

color-code depending on TChla (in red: high concentrations SD1 to SD7, Melanesian archipelago), in black: median TChla: medium concentrations, SD8 to SD11 around Fiji Islands, in blue low concentrations SD12 to SD15 including LDC (Table 1) with the frontal station LDB in green.

Figure 4. Sections from 0 to 150 m of a) Abundance of Fiber Tricho Like$_{Trichodesmium}$ (N.m^{-3}), b) Zeaxanthin concentration (mg.m^{-3}), c) TChla concentration (mg.m^{-3}) by HPLC-LOV (J. Ras) d) Surface maps of TChla HPLC-NASA (mg.m^{-3}) and e) PE > 10 µm by spectrofluorimetry (mg.m^{-3}). Short transects data from pump samples (5 m depth) at 165°E and at 170°W are included. Ocean Data View sections Schlitzer, R., Ocean Data View, http://odv.awi.de, 2016. Station numbers along the transect are indicated.

Figure 5. Surface values along the transect of a) DV-Chla (mg m^{-3}) and different fractions of MV-Chla (mg m^{-3}) using HPLC and flow cytometry (Chla-nano+micro), Chla-Syn+Peuk) allowing to extract Chla from *Trichodesmium* (Chla-Trich.), b) Zeaxanthin (mg m^{-3}) (left axis) and % of TChla and % zeaxanthin by *Trichodesmium* (right axis). All pigments from HPLC NASA. Station numbers along the transect are indicated on the X axis. Main longitudes (E, W) are indicated above.

Figure 6. Surface values along the transect of the trichome concentration from visual counts and estimated from the Chla, zeaxanthin and PE of *Trichodesmium* (Trich.(Chla), Trich(zea), Trich.(PE>10µm)) (N L^{-1}) (left axis) and of FTL$_{Trichodesmium}$ abundance (colony counts by UVP5) at 10 m (N L^{-1}) (right axis). Station numbers along the transect are indicated on the X axis. Main longitudes (E and W) are indicated above.

Figure 7. Correlations between the a) Trichome concentration estimated from PE > 10 µm or Chla(Tri) and the FTL$_{Trichodesmium}$ abundance (colony counts by UVP5) (N L^{-1}) b) Chla (Trich.) vs Trichome concentration from visual counts (N L^{-1}).

Figure 8. IOPS: a) Backscattering spectrum (log (b_{bp} (m^{-1})) vs log (wavelength) measured by a HOBILABS Hydroscat-6 in *Trichodesmum* rich waters showing troughs at the absorption wavelengths (in red) and at an oceanic station of the Diapalis 2001-2003 data basis with the same H6, c) Section from 0-150m of log(b_{bp} (555)). Ocean Data View sections Schlitzer, R., Ocean Data View, http://odv.awi.de, 2016.

Figure 9. IOPS (continued): a) *In situ* absorption spectrum of *Trichodesmum* rich waters as measured by the filter technique showing MAA's absorption at 330 and 360 nm wavelengths and b) idem for low *Trichodesmium*, c) OUTPACE section of a_P(330) (upper panel), and a_P(442) (lower panel). Ocean Data View sections Schlitzer, R., Ocean Data View, http://odv.awi.de, 2016.

Figure 10. a) Relationship (Log/Log) between a_P (330) and the FTL$_{Trichodesmium}$ abundance (colony counts by UVP5) (N.m^{-3}) at all station/ depths (0-150m) b) Vertical distributions of a_P(330)/a_P(676) at all stations, c) OUTPACE sections from 0-150m of the surface ratio a_P(330)/a_P(676), and trichome concentration (visual counts) along the transect. Station numbers along the transect are indicated on the X axis. Main longitudes (E and W) are indicated above.

Figure 11. Correlations between the Chla (fluorimetry) and the ratio of $nL_w(\lambda)/nL_w$(565 nm)

© Author(s) 2018. CC BY 4.0 License.

at different UV and visible wavelengths. Equations and determination coefficient (r^2) of the power law are indicated for each wavelength a) 305, b) 325, c) 340, d) 380, e) 412, f) 443, and g) 490 nm). All stations of the OUTPACE and BIOSOPE transect are reported. In black, OUTPACE, in blue, BIOSOPE

Figure 12. Principal component analysis (PCA), based on Pearson's correlation matrices, computed on the $nL_w(\lambda)$ and TChla for OUTPACE (a, b) and for BIOSOPE) (c, d). For OUTPACE (a,b) all surface data were used, including 7 days at LDA, LDB, LDC (n=37). For BIOSOPE, all surface data (n = 17) were used (c,d).

Biogeosciences Discuss., https://doi.org/10.5194/bg-2017-570
Manuscript under review for journal Biogeosciences
Discussion started: 15 January 2018
© Author(s) 2018. CC BY 4.0 License.

971

972 APPENDIX A: AOPS measurements and processing

973 For in-water sensors, the Full- Width Half-Maximum (FWHM) of the channels was 2
974 nm for 305, 325 and 340 nm, and 10 nm for 380, 412, 443, 490 and 565 nm. For in-air
975 sensors, the FWHM of the channels was 2 nm for 305, 325 and 340 nm, 10 nm for 380 nm,
976 and 20 nm for 412, 443, 490 and 565 nm. The MicroPro free-fall profiler was operated from
977 the rear of the ship and deployed 20-30 m away to minimize the shadowing effects and
978 disturbances of the ship. Surface irradiance (Es(λ), in µW cm^{-2} nm^{-1}), which is equivalent to
979 the downward irradiance just above the sea surface (Ed(0+, λ)), was simultaneously measured
980 at the same channels on the ship deck using other OCR-504 sensors to account for the
981 variations of cloud conditions during the cast. Details of cast measurements are as follows.
982 Rejection was the case at SD6 (2^{nd} profile), during the long duration stations LDC (2^{nd} profile
983 day1, 2^{nd} profile day2, 1^{st} profile day3, 2^{nd} profile day5) and LDA (1st profile DAY5), LDB
984 (2^{nd} profile DAY3) an LDC (2^{nd} profile DAY1, 2^{nd} profile DAY2, 2^{nd} profile DAY5). In total,
985 all stations were characterized by at least 1, 2 profiles and sometimes 3 profiles. Only 2 values
986 of nLw(λ) at 305 nm (SD5 and SD14) showed some suspicious radiometric values among the
987 30 nLw profiles.
988 Ed(λ) was taken from the OCR Hyperpro values from 400 to 700 nm and then
989 integrated using the formula (Tedetti et al., 2007, eq. 1) where $Ed_{,PAR(Z)}$ is the downward
990 irradiance in the spectral range of PAR at depth Z (quanta cm^{-2} s^{-1}), λ is the wavelength
991 (nm), h is the Planck's constant (6.63.10-34 J s), c is the speed of light in the vacuum (3.108
992 m s-1) and Ed(Z, λ) is the downward irradiance at depth Z (mW cm^{-2} nm^{-1}). Downward
993 attenuation coefficient was determined in accordance with their eq. 2, where Ed(0-,λ) is the
994 downward irradiance beneath the surface. Because of the wave-focusing effects leading to
995 fluctuations in in-water irradiance near the surface, irradiance data of the first meters were
996 omitted from the calculation and Ed(0-,λ) was theoretically computed from deck
997 measurements as in their eq. 3, where alpha (0.043) is the Fresnel reflection albedo for
998 irradiance from sun and sky.
999 The diffuse attenuation coefficient for upward irradiance was determined from the
1000 slope of the linear regression of the log-transformed upward radiance versus depth in
1001 accordance with the equation between Lu(Z1, λ) and Lu(Z2, λ) the upward radiances (µW
1002 cm^{-2} sr^{-1}) at depths Z1 and Z2 (m), respectively (Tedetti et al., 2010). As for Kd(λ), the depth

© Author(s) 2018. CC BY 4.0 License.

interval within the upper water column used for the KL(λ) determination was chosen from a visual examination of each log-transformed profile and was typically 5, 10, 15, 20, or 30 m, depending on the stations and wave bands. The determination coefficients (r_2) of the KL(λ) calculation were >0.98. Water-leaving radiance (Lw(λ) in µW cm^{-2} sr^{-1}) was then derived (their equation 2) where Lu(0-, λ) is the upward radiance beneath the sea surface computed by extrapolating Lu(Z, λ) to the sea surface from KL(λ) and equation (1), t (0.975) is the upward Fresnel transmittance of the air-sea interface, and n (1.34) is the refractive index of water. Normalized water-leaving radiance (nLw(λ) in µW cm^{-2} sr^{-1}) was determined by the formula (equation 3) by dividing the water-leaving radiance (Lw(λ) by Es(λ) the surface irradiance and multiplying by F0(λ) the solar irradiance at the top of the atmosphere, at the mean Earth-Sun distance (mW cm^{-2}). F0(λ) data in the ranges 305 –340 nm and 380 – 565 nm were used from Thuillier et al. [1997, 1998], respectively as in Tedetti et al. (2010).

APPENDIX B

Table 1. Pump sampling between SD3 and SD4 in the Melanesian Archipelago for calibrating the SIMBADA instrument during the OUTPACE cruise. HPLC from NASA.

SIMBADA survey	Longitude (E)	Latitude (S)	TChla-NASA (mg.m-3)
Surf 1 4/03/16	166.978	-19.704	0.5785
Surf 2 4/03/16	166.6956	-19.837	0.384
Surf 3 4/03/15	166.696	-19.847	0.357
Surf 4 4/3/15	166.779	-19.869	0.3135
Surf5 4/03/15	166.956	-19.896	0.3185
Surf 6 4/03/15	167.167	-19.923	0.397
Surf 7 4/03/15	167.383	-19.955	0.326
Surf 8 4/03/15	167.639	-19.977	0.2615
Surf 9 5/03/15	167.817	-21.447	0.269
Surf 10 6/03/15	169.445	-21.497	0.19

Biogeosciences Discuss., https://doi.org/10.5194/bg-2017-570
Manuscript under review for journal Biogeosciences
Discussion started: 15 January 2018
© Author(s) 2018. CC BY 4.0 License.

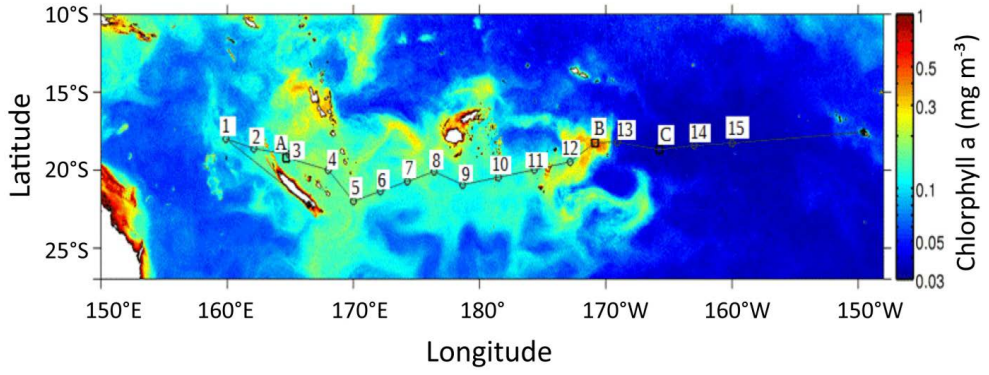

Fig. 1

Biogeosciences Discuss., https://doi.org/10.5194/bg-2017-570
Manuscript under review for journal Biogeosciences
Discussion started: 15 January 2018
© Author(s) 2018. CC BY 4.0 License.

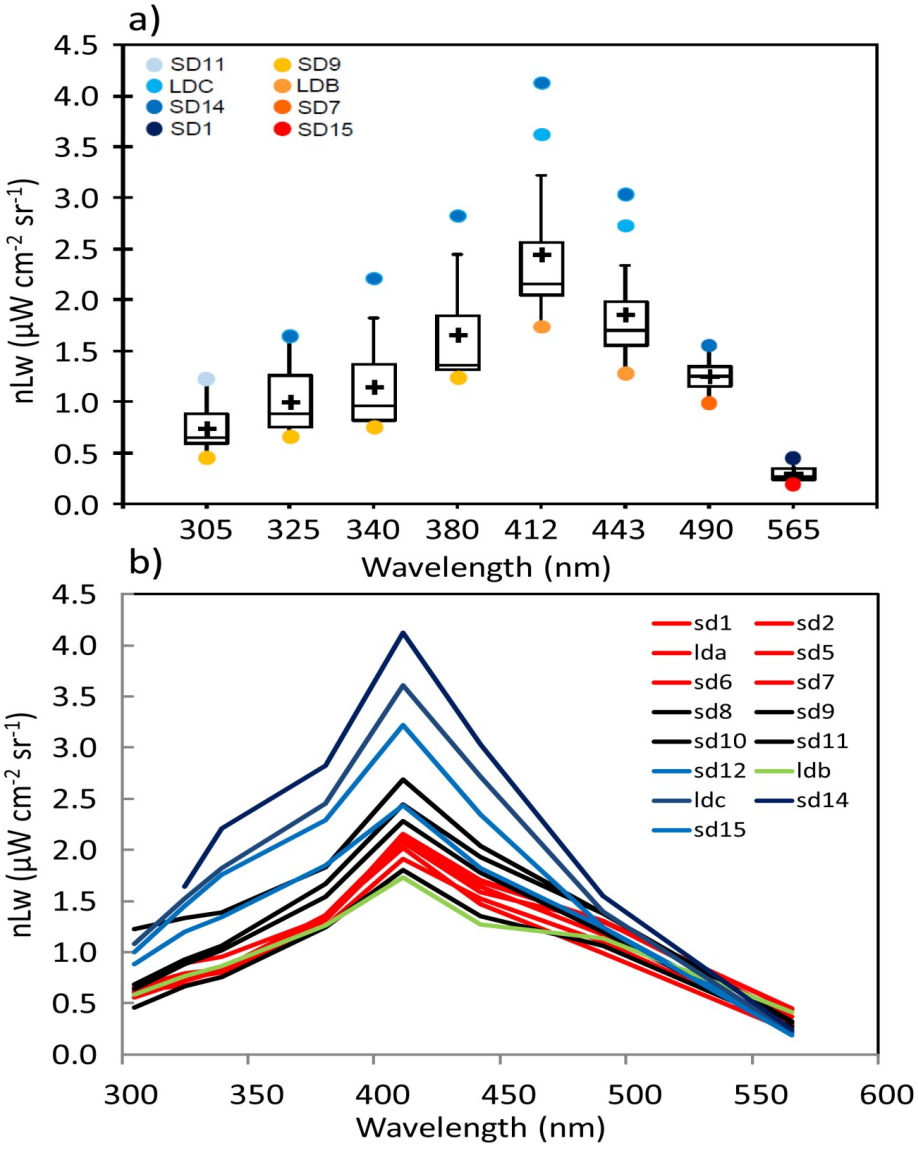

1042

1043

1044 **Fig. 2**

1045

1046

Biogeosciences Discuss., https://doi.org/10.5194/bg-2017-570
Manuscript under review for journal Biogeosciences
Discussion started: 15 January 2018
© Author(s) 2018. CC BY 4.0 License.

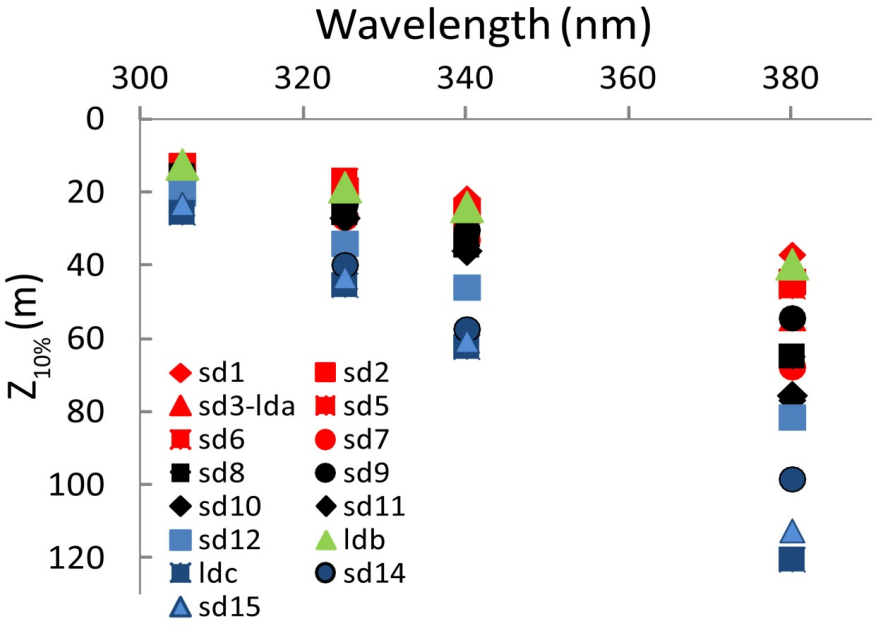

Fig. 3

Biogeosciences Discuss., https://doi.org/10.5194/bg-2017-570
Manuscript under review for journal Biogeosciences
Discussion started: 15 January 2018
© Author(s) 2018. CC BY 4.0 License.

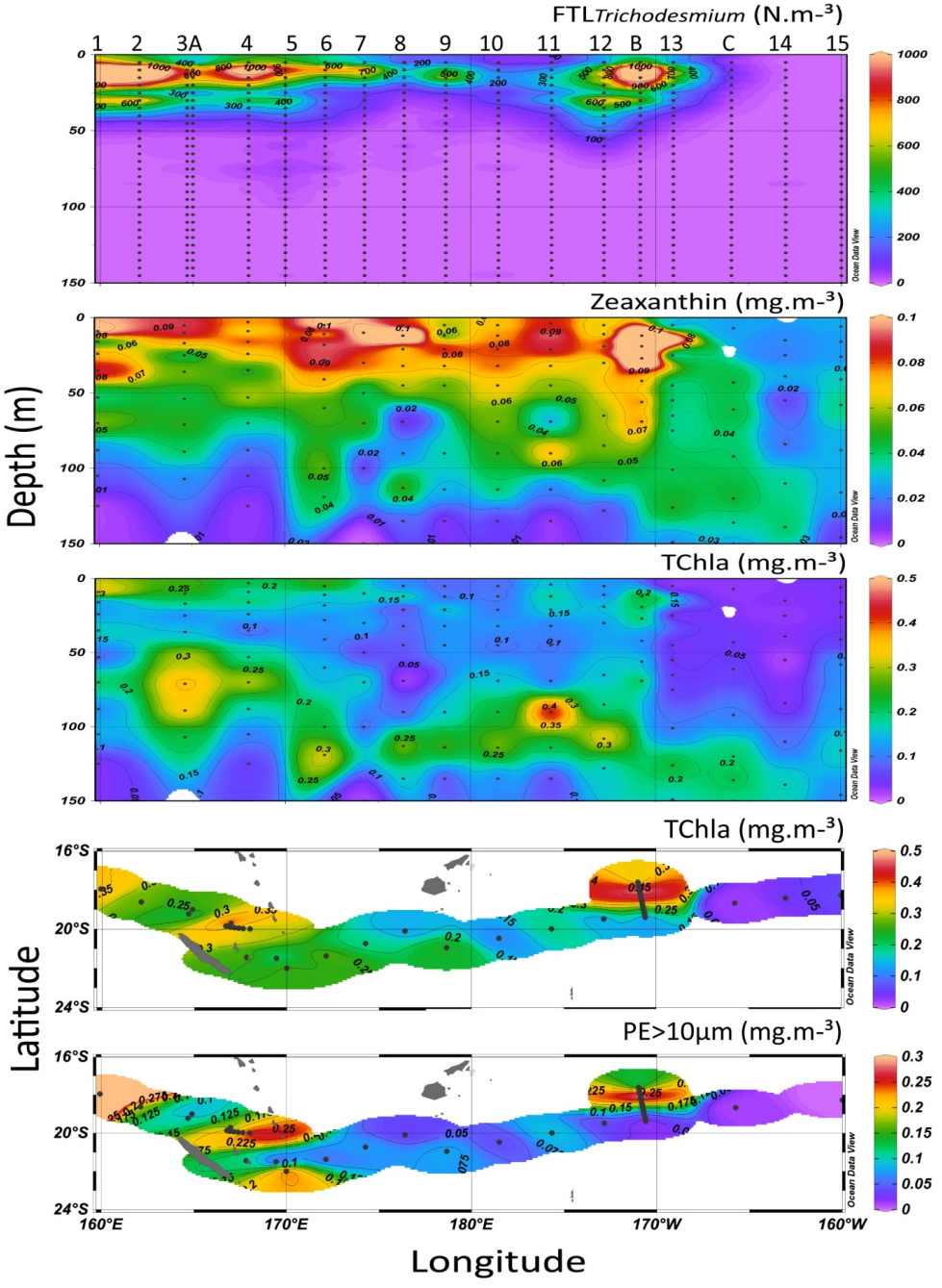

1060 **Fig. 4**

1061

Biogeosciences Discuss., https://doi.org/10.5194/bg-2017-570
Manuscript under review for journal Biogeosciences
Discussion started: 15 January 2018
© Author(s) 2018. CC BY 4.0 License.

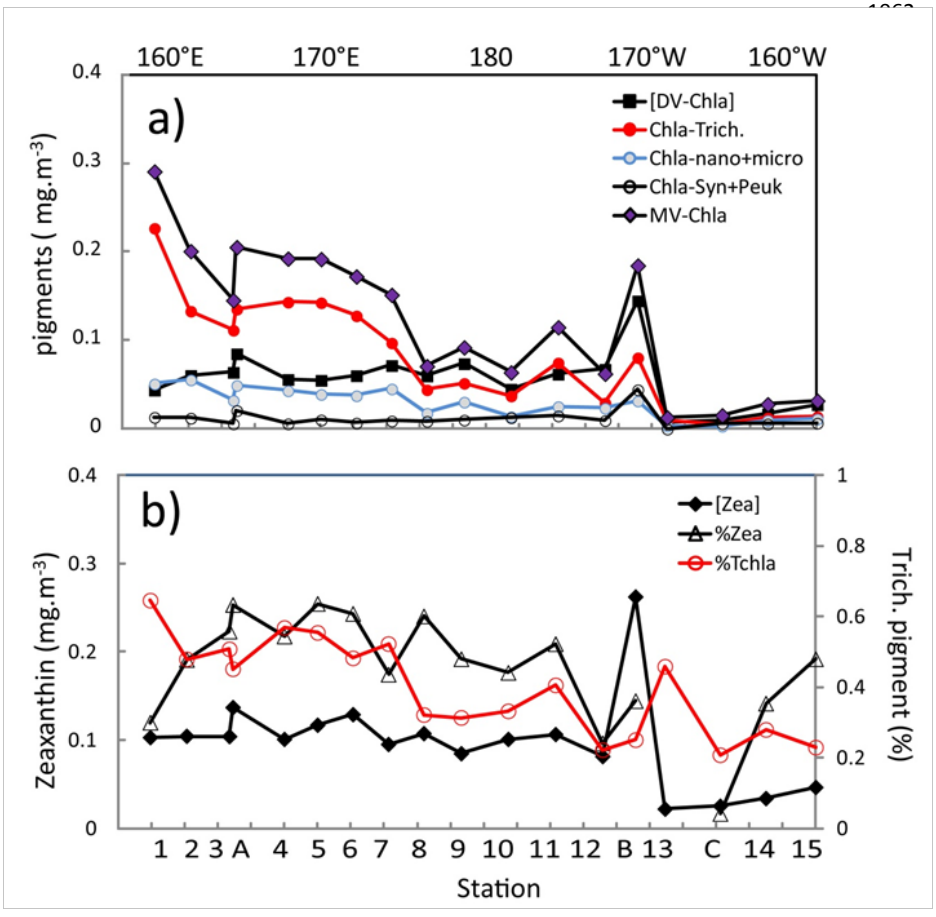

Fig. 5

Biogeosciences Discuss., https://doi.org/10.5194/bg-2017-570
Manuscript under review for journal Biogeosciences
Discussion started: 15 January 2018
© Author(s) 2018. CC BY 4.0 License.

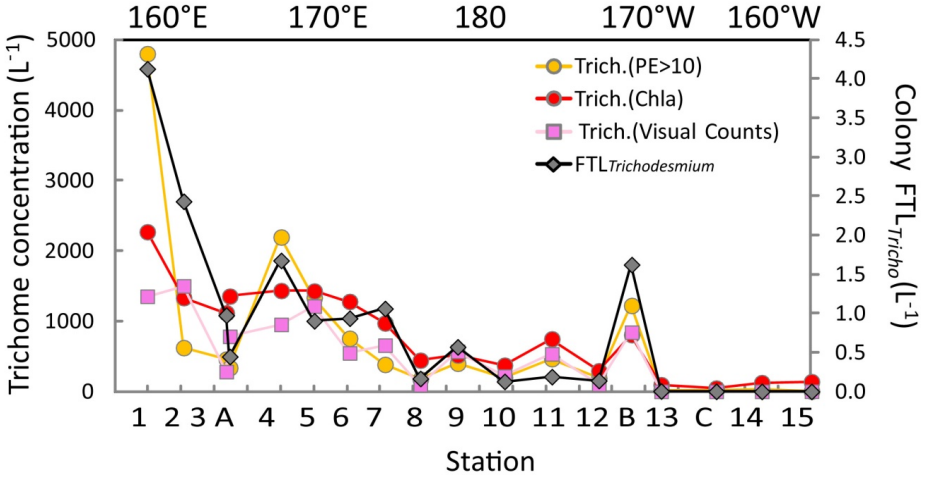

Fig. 6

Biogeosciences Discuss., https://doi.org/10.5194/bg-2017-570
Manuscript under review for journal Biogeosciences
Discussion started: 15 January 2018
© Author(s) 2018. CC BY 4.0 License.

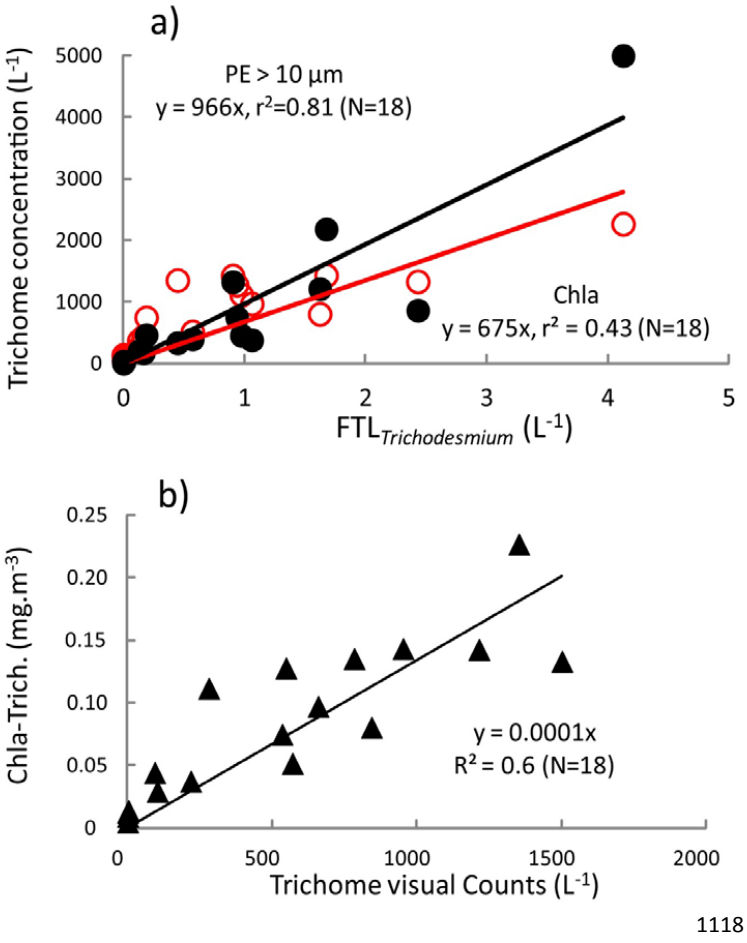

Fig. 7

Biogeosciences Discuss., https://doi.org/10.5194/bg-2017-570
Manuscript under review for journal Biogeosciences
Discussion started: 15 January 2018
© Author(s) 2018. CC BY 4.0 License.

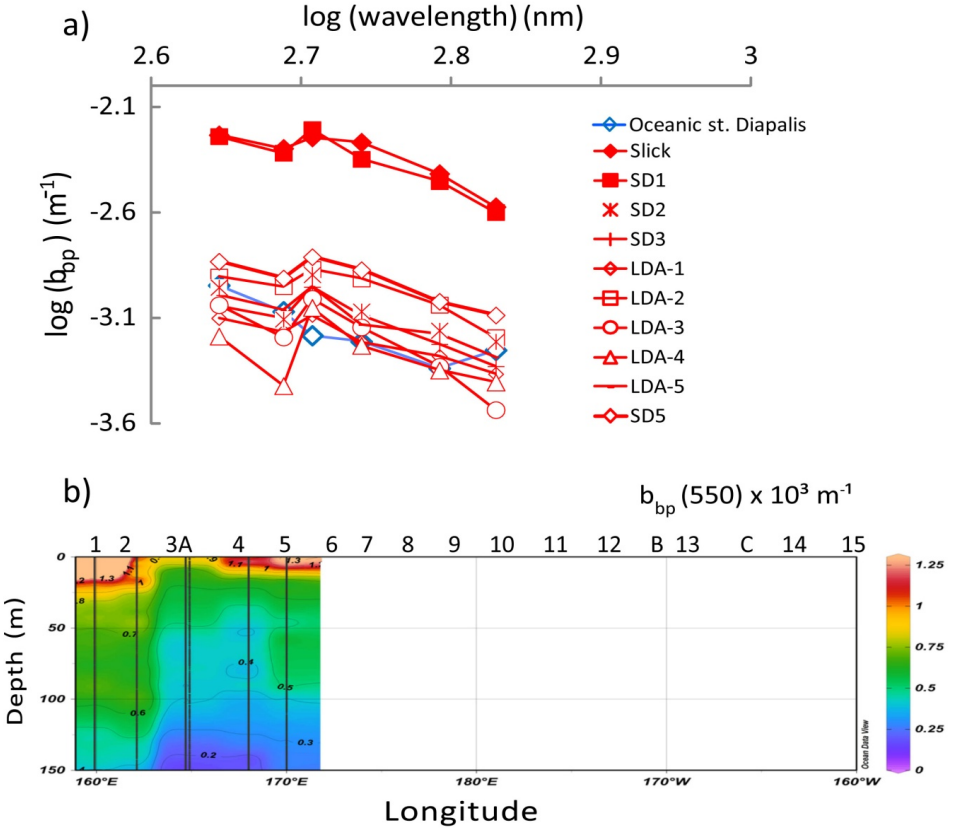

1127

1128 **Fig. 8**

1129

1130

Biogeosciences Discuss., https://doi.org/10.5194/bg-2017-570
Manuscript under review for journal Biogeosciences
Discussion started: 15 January 2018
© Author(s) 2018. CC BY 4.0 License.

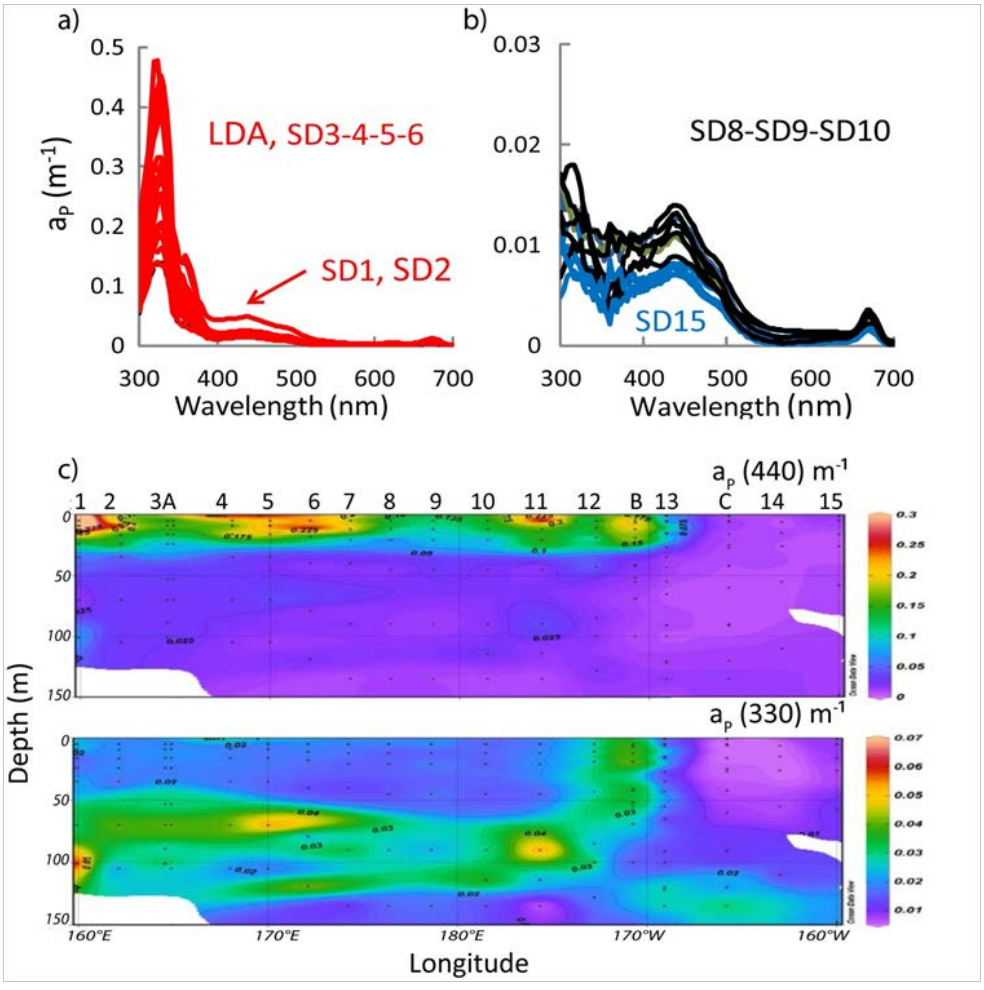

1131

1132

1133

1134 **Fig. 9**

1135

1136

Biogeosciences Discuss., https://doi.org/10.5194/bg-2017-570
Manuscript under review for journal Biogeosciences
Discussion started: 15 January 2018
© Author(s) 2018. CC BY 4.0 License.

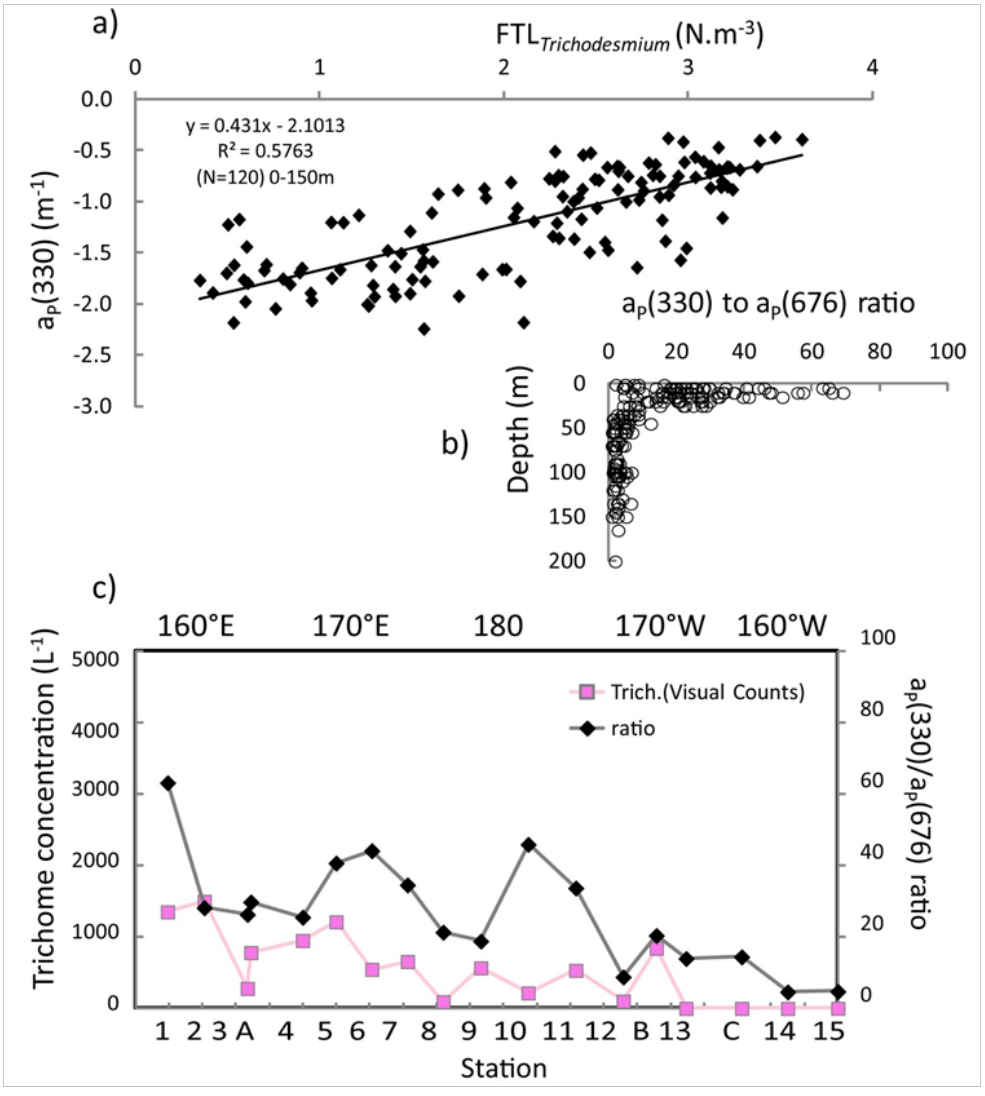

Fig. 10

Biogeosciences Discuss., https://doi.org/10.5194/bg-2017-570
Manuscript under review for journal Biogeosciences
Discussion started: 15 January 2018
© Author(s) 2018. CC BY 4.0 License.

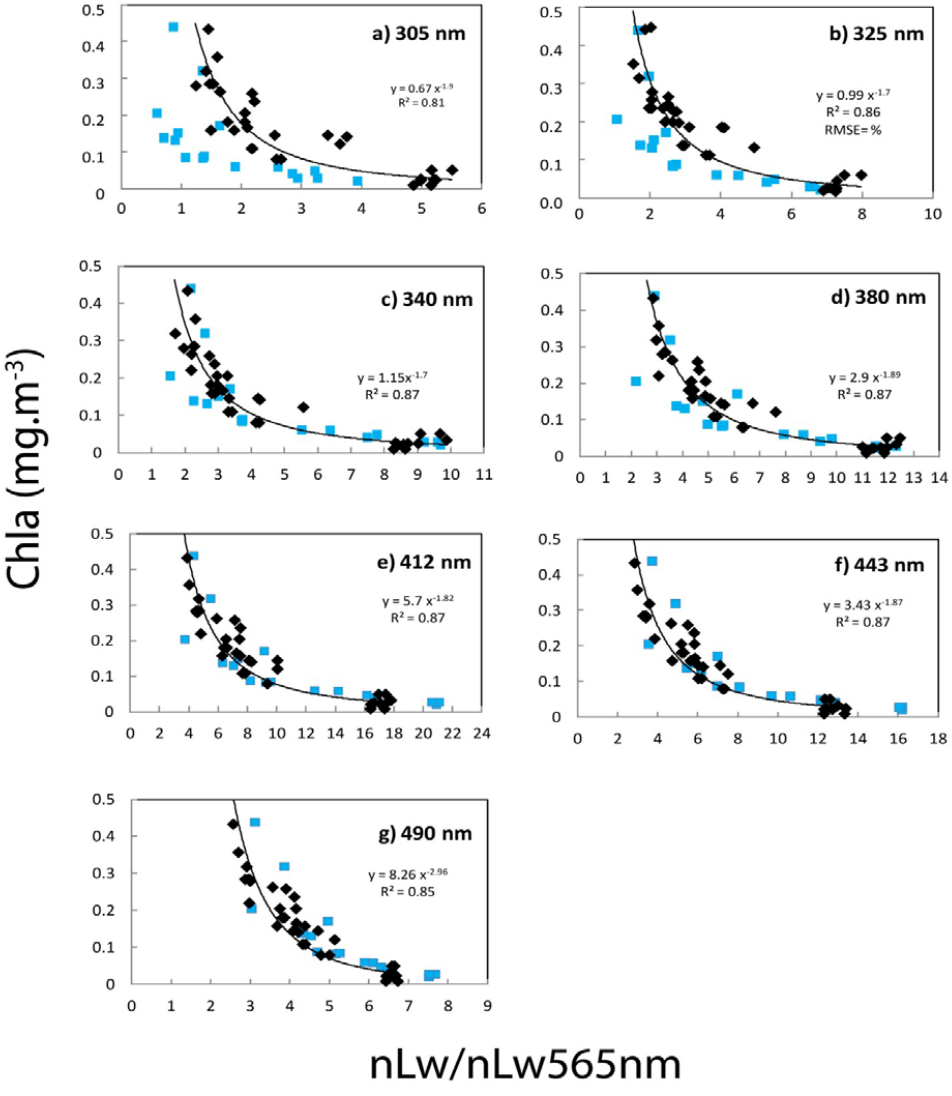

1143

1144 **Fig. 11**

Biogeosciences Discuss., https://doi.org/10.5194/bg-2017-570
Manuscript under review for journal Biogeosciences
Discussion started: 15 January 2018
© Author(s) 2018. CC BY 4.0 License.

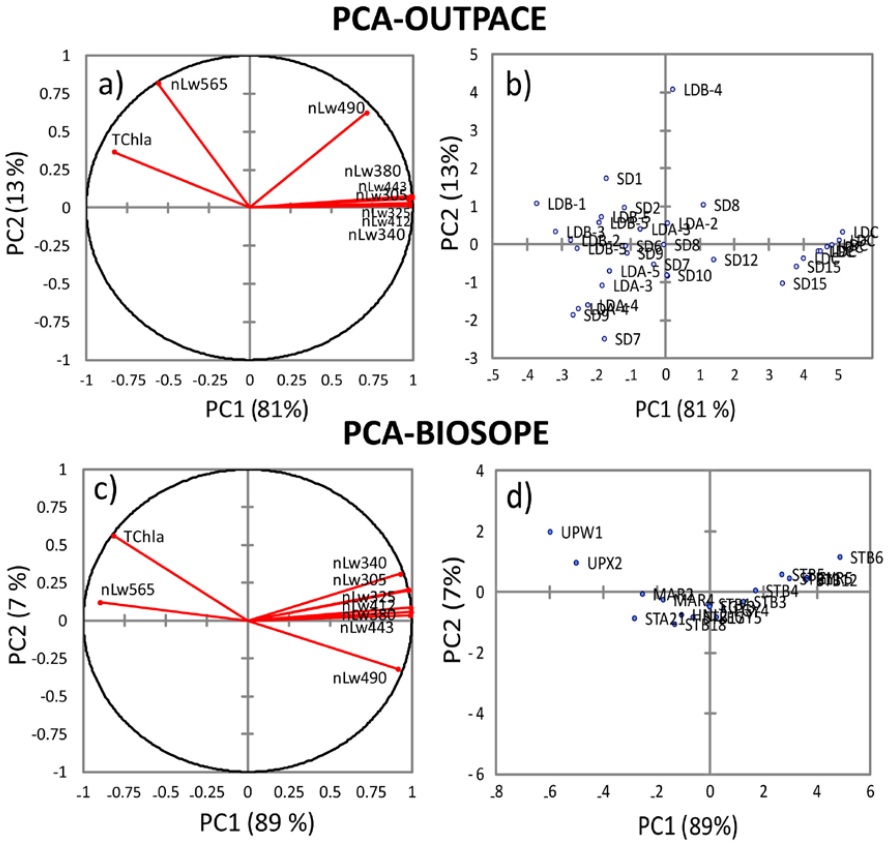

1145

1146

1147

1148

1149

1150

1151 **Fig. 12**

1152